Establishment of an experimental rat model of tacrolimus-induced kidney injury and protective effects of hypoxia-inducible factor prolyl hydroxylase (HIF-PHD) inhibitors

付, 饒

出版情報：Kyushu University, 2022, 博士（臨床薬学）, 課程博士
バージョン：
権利関係：

Establishment of an experimental rat model of tacrolimus-induced kidney injury and protective effects of hypoxia-inducible factor prolyl hydroxylase (HIF-PHD) inhibitors

2022

Department of Clinical Pharmacology and Biopharmaceutics,
Graduate School of Clinical Pharmacotherapy, Kyushu University

Rao Fu

Contents

Abbreviations

AKI	acute kidney injury
ANOVA	analysis of variance
AUC	area under the concentration-time curve
BUN	blood urea nitrogen
CKD	chronic kidney disease
DMSO	dimethyl-sulfoxide
EMT	epithelial-mesenchymal transition
GAPDH	glyceraldehyde 3-phosphate dehydrogenase
HE	hematoxylin and eosin
HIF	hypoxia-inducible factor
HIF-PHD	hypoxia-inducible factor prolyl hydroxylase
HRP	horseradish peroxidase
IL	interleukin
I/R	ischemia reperfusion
K	potassium
KIM-1	kidney injury molecule 1
MCP-1	monocyte chemotactic protein 1
Mg	magnesium
MTS	Masson's trichrome

NFAT	nuclear factor of activated T cells
PAS	periodic acid-Schiff
PBS	phosphate buffer saline
PVDF	polyvinylidene fluoride
ROX	roxadustat
Scr	serum creatinine
SDS-PAGE	sodium dodecyl sulfate-polyacrylamide gel electrophoresis
TAC	tacrolimus
TDM	therapeutic drug monitoring
TGF-β	transforming growth factor-β
T-PER	tissue protein extraction reagent
α-SMA	α-smooth muscle actin

Introduction

On December 23, 1954 in Boston, the first successful human kidney transplantation performed between identical twins brought hope to patients with end-stage renal disease[1]. Currently, kidney transplantation is considered as the best therapy choice for end-stage renal disease, especially in conjunction with the strong immunosuppressive abilities of calcineurin inhibitors, such as tacrolimus (TAC), which was discovered in the 1980s[2, 3]. TAC is the cornerstone of most immunosuppressive regimens in kidney transplantation. With TAC use, the survival rate of transplants 1 year after kidney transplantation is about 90%, with the incidence of acute rejection being less than 20%[4-6].

The immunosuppressive properties of TAC result from inhibition of calcineurin, which is the key protein phosphatase for the activation of T cells. TAC prevents the dephosphorylation of nuclear factor of activated T cells (NFAT) proteins by binding to cytosolic immunophilins, which, in turn, bind to and inhibit calcineurin, which inhibits NFAT activity[7, 8]. An NFAT has two subunits, one of which is confined to the cytoplasm, while the other has predominantly nuclear localization. In resting T cells, NFAT proteins are hyperphosphorylated and retained in the cytosol. The activation of T-cell receptors activates calcineurin, which dephosphorylates NFAT, allowing for its translocation to the nucleus,

where it activates the expression of a range of genes[9]. The calcineurin–NFAT pathway was initially described in T cells, where NFAT acts as a master regulator of lymphocyte development and expression of pro-inflammatory cytokines, such as interleukin (IL)-2, IL-3, IL-4, interferon-γ, and tumor necrosis factor-α. The classic calcineurin-NFAT signaling pathway can be described as follows. When the receptors accept an antigen, phospholipase C-γ is activated, which hydrolyzes phosphatidylinositol-4,5- bisphosphate into inositol-1,4,5-trisphosphate and diacylglycerol. Next, inositol-1,4,5-trisphosphate binds to specific receptors on the endoplasmic reticulum and drives Ca^{2+} release from the endoplasmic reticulum into the cytoplasm, which triggers the opening of Ca^{2+} release-activated Ca^{2+} channels. As a result of the increased intracellular Ca^{2+} levels, the calcineurin enzyme becomes active and dephosphorylates NFAT, allowing for the translocation of NFAT into the nucleus and the subsequent regulation of gene expression[10]. NFAT signaling was later identified in other immune cells as well, including B cells, dendritic cells, and megakaryocytes[11, 12]. TAC has, therefore, been regarded as an inhibitor of immune-cell functions.

Oral bioavailability of TAC is weak (10%–20%) and varies dramatically among individuals, ranging from 5% to 90%, mainly due to intestinal P-glycoprotein efflux and metabolism by intestinal and hepatic cytochrome 450 3A[13]. In conjunction with the narrow therapeutic range of TAC (5–20 ng/mL), underexposure increases the risk of rejection, whereas overexposure increases the risk of adverse effects (such as nephrotoxicity, neurotoxicity, infections,

malignancies, hypertension, diabetes, and gastrointestinal complaints) therefore,therapeutic drug monitoring (TDM) of TAC is considered to be essential for patient management and determining individualized dosage adjustments for the prevention of post-transplant rejection. Despite the large variation in TAC pharmacokinetics, the area under the concentration-time curve (AUC) has a nearly linear relationship with the trough blood concentration among kidney transplant patients; therefore, AUC determination is proposed as the best TDM option early after transplantation, at the time of immunosuppression minimization, for special populations, and specific clinical situations[14].

Despite best efforts to reduce the side effect of TAC, such as TAC minimization and withdrawal at early time-point its long-term use still causes chronic, structural, progressive, and irreversible nephrotoxicity, which is thought to be the primary cause of chronic allograft dysfunction. Previous clinical studies have demonstrated TAC-related nephrotoxicity in 16.1% of patients, at six months post-kidney transplantation[15]. Kidney allograft function is an important predictor of graft survival. At 5 years post-transplantation, 54% renal allografts sustained major histologic injury, which increased to 82% at 10 years[16]. TAC causes kidney injury, including arteriolar hyalinosis, tubular atrophy, interstitial fibrosis, and glomerulosclerosis, which can lead to irreversible kidney dysfunction[17]. Renal interstitial fibrosis is a typical feature of TAC-induced nephrotoxicity, and renal fibrosis represents the common pathway of nearly all

chronic and progressive nephropathies, limiting tissue regeneration potential, thereby further reducing kidney function[18]. At present, attempts to elucidate the mechanism underlying TAC-induced renal injury have been hindered by the need for a suitable animal model.

Hypoxia is one of the most common causes of kidney injury, which plays a key role in the pathological condition of various kidney diseases. Tubular epithelial cells are rendered particularly prone to hypoxic injury, due to their high metabolic activity and large oxygen demand[19-21]. Hypoxia causes tubular cell injury and death. Damaged tubular cells worsen glomerular lesions *via* tubular obstruction and maladaptive tubuloglomerular feedback, thereby inducing interstitial fibrosis. Glomerular injury and interstitial fibrosis then aggravate tubular hypoxia, resulting in a vicious cycle and advancement of chronic kidney disease (CKD)[22].

Hypoxia-inducible factor (HIF) is a well-known master mediator of hypoxia-adaptive responses in a variety of pathophysiological processes in the kidney diseases[23]. HIF are transcription factors that mediate cellular adaptation to hypoxia by regulating the gene expression of various proteins that mediate glycolysis, angiogenesis, erythropoiesis and cell survival[24]. There are two major HIF-α isoforms, HIF-1α and HIF-2α, both of which dimerize with the same β-subunit to form functional HIF-1 and HIF-2 transcription factors, respectively. In the presence of oxygen, HIF-α subunits are hydroxylated on specific proline residues by a family of HIF prolyl hydroxylase (HIF-PHD) enzymes comprising

of three isozymes: PHD1, PHD2, and PHD3. This hydroxylation enables binding of the von Hippel-Lindau protein, a component of an E3 ubiquitin ligase, which ubiquitinates HIF-α to target it for proteasomal degradation. HIF-PHD enzymes require α-ketoglutarate and oxygen as cosubstrates. Thus, when oxygen levels fall, the activity of HIF-PHD enzymes decreases, causing HIF-α subunits to accumulate and dimerize with HIF-β to form functional transcription factors. This process induces adaptive changes in gene expression that either enhance oxygen delivery (*e.g.*, erythropoiesis) or promote survival in a hypoxic environment[25]. Increasing evidence indicates that HIF is a pivotal regulator of kidney fibrosis under various pathological conditions.

Using the rat remnant kidney model to induce renal fibrosis, the pharmacological activation of HIF attenuated renal injury and tubulointerstitial fibrosis[26-29]. Another study showed that global activation of HIF repressed fibrogenesis in mice subjected to unilateral ureteral obstruction[30]. In addition, in a mouse model of cyclosporin A-induced toxicity, activated HIF improved renal function *via* inhibition of apoptosis, inflammation, and fibrosis[31].

Inhibition of PHD results in accumulation of HIFs and stimulates HIF-dependent gene expression. Roxadustat (ROX), also known as FG-4592, is a first in class, potent PHD inhibitor that is used as a novel treatment for anemia of CKD. Some studies have reported that in acute kidney injury (AKI) mouse models, ROX improved kidney function and reduced AKI-induced renal fibrosis, *via* angiogenesis and activation of the Akt/GSK-3β/Nrf2 pathway[32, 33]; however, the

effects of ROX in the TAC-induced nephropathy rat model are unknown.

Based on the above literature, in Chapter 1, we report a new method for developing TAC-induced nephropathy with renal interstitial fibrosis in a shorter time. Thereafter in Chapter 2, we discuss the effects of roxadustat in the TAC-induced nephropathy rat.

Catalog of treatises

Establishment of an experimental rat model of tacrolimus-induced kidney injury accompanied by interstitial fibrosis

Rao Fu, Soichiro Tajima, Tomohiro Shigematsu, Mengyu Zhang, Nobuaki Egashira, Ichiro Ieiri, and Satohiro Masuda

Toxicology Letters. 2021; 341:43–50.

Chapter 1. Establishment of an experimental rat model of tacrolimus-induced kidney injury accompanied by interstitial fibrosis

1. Introduction

The long-term use of TAC can irreversibly affect all three compartments of the kidneys: the vessels (arteriolar hyalinosis), tubulo-interstitium (tubular atrophy and interstitial fibrosis), and glomeruli (thickening and fibrosis of Bowman's capsule and focal segmental or global glomerular sclerosis)[34]. Reducing nephrotoxicity incidence requires understanding the underlying pathogenic factors and mechanisms. It is a multifactorial process that begins with acute local inflammation, oxidative stress, renal vasoconstriction, and ends with a chronic fibrogenic response after prolonged TAC use[35]. Renal interstitial fibrosis is a typical feature of TAC-induced nephrotoxicity, and represents the common pathway of nearly all chronic and progressive nephropathies, limiting tissue regeneration potential, thereby further reducing kidney function[18].

The mechanism of TAC-induced renal fibrosis has been extensively studied, and partially elucidated to involve reactive oxygen species[36, 37], transforming growth factor-β (TGF-β)[38], and the renin-angiotensin system[39, 40]; however, attempts to elucidate the mechanism underlying TAC-induced renal injury accompanied by interstitial fibrosis have been hindered by the need for a suitable

animal model. Previously reported experimental rat models of TAC-induced nephropathy either require long-term treatment or have effects other than those of TAC. In one study, rats treated with 0.6 mg/kg TAC per day for nine weeks exhibited significantly decreased renal function, but no observable histological changes[41]. In another study, no significant histological changes were observed after rats were orally administered a high dose of TAC (approximately 6 mg/kg per day) for six weeks[42]. In contrast, a sodium-deficient rat model showed typical physiological and histological features of TAC-induced kidney toxicity after four weeks of TAC administration[43]. Thus, in the present study, we investigated whether administration of TAC for two weeks post kidney ischemia-reperfusion (I/R) could produce an experimental rat model of renal injury with interstitial fibrosis.

2. Materials and Methods

2-1 Animals and Drugs

Male Wistar rats purchased from SLC (Shizuoka, Japan) were housed under standard conditions with water and food ad libitum. Experiments were performed in accordance with the Guidelines for Animal Experiments of Kyushu University. All experimental protocols were approved by the Animal Research Committee of the Graduate School of Medicine, Kyushu University (approval number: A30-029-0).

The purchased rats were housed under controlled temperatures of 25 ± 1 °C and a 12 h/12 h light/dark cycle, with water and food *ad libitum*. Before drug administration, renal I/R injury was performed according to a previously published protocol[44]. Rats were anesthetized by means of isoflurane inhalation, with a 4% dose for induction and a 1.5% dose for maintenance. The abdominal cavity was then exposed using midline laparotomy. Subsequently, both renal pedicles were cross-clamped for 45 min. During ischemia, the rats were hydrated with saline and maintained at 37°C using heating plates. Renal clamps were removed after 45 min, and all incisions were closed. After surgery, the animals were placed on the heating plates until recovery from anesthesia, and then moved to cages with free access to water and standard rat chow.

The rats (n = 30) were randomly divided into four groups: (1) sham group,

sham operation on day 1 and treatment with saline for 14 d (n=7); (2) IR group, renal I/R injury on day 1 and treatment with saline for 14 d (n=7); (3) TAC group, sham operation on day 1 and treatment with TAC (5mg/kg per day) for 14 d (n=9); (4) TAC+IR group, renal I/R injury on day 1 and treatment with TAC (5mg/kg per day) for 14 d (n=7).

TAC (0.26–0.29 mL; 5 mg/kg; Prograf; Astellas Pharma Inc., Tokyo, Japan) was subcutaneously administered to the backs of the TAC and TAC+IRI groups, once daily for two weeks. In addition, 0.26–0.29 mL of saline was subcutaneously administered to the sham and IRI groups, once daily for two weeks.

All rats were sacrificed on day 15. After the rats were anesthetized, whole blood and serum samples were collected by means of cardiac puncture, following which the kidneys were harvested. The right kidney from each animal was cut into half. One-half of each kidney was snap-frozen in liquid nitrogen and subsequently stored at −80°C for use in western blot. The other half was fixed in Carnoy's solution for further analysis. Figure 1 shows a schematic representation of the experimental procedure.

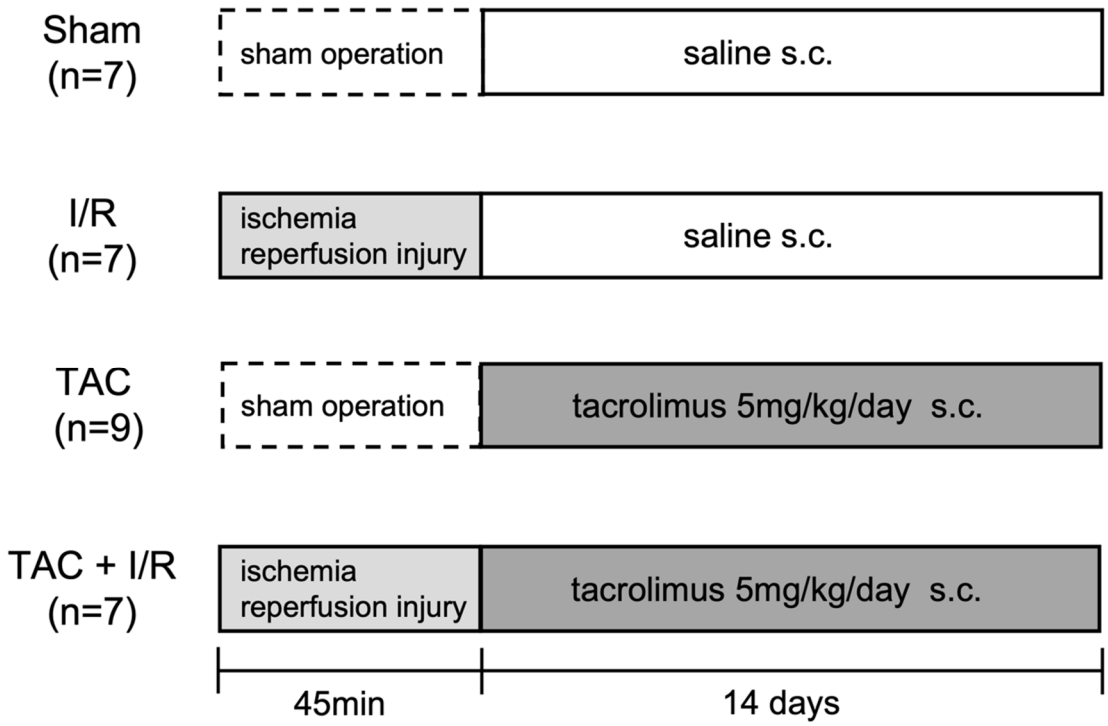

Figure 1. Schematic illustration of the experimental protocol.

Sham group, sham-operated in kidney and treated with saline for 14 d; I/R group, bilateral kidney ischemia induced at day 1 for 45 min and treated with saline for 14 d; TAC group, sham-operated in kidney and treated with tacrolimus (5mg/kg/day) for 14 d; TAC+I/R group, bilateral kidney ischemia induced at day 1 for 45 min and treated with tacrolimus (5mg/kg/day) for 14 d. The rats were sacrificed under anesthesia on day 15, following which the blood samples and tissue specimens were obtained for further analyses.

I/R, ischemia reperfusion; s.c., sub-cutaneous administration; TAC, tacrolimus.

2-2 Evaluation of renal function

Rat whole blood was centrifuged for 10 min at 3000 rpm, following which the upper serum was collected and stored at –80°C until further use. Serum creatinine (Scr) and blood urea nitrogen (BUN) were measured to assess renal function using the LabAssay™ Creatinine kit (catalog no: 290-65901; Wako Pure Chemical Industries Ltd., Osaka, Japan) and Wako Urea N B-kit (catalog no: 279-36201; Wako Pure Chemical Industries Ltd.), respectively. Measurement of serum magnesium (Mg), serum potassium (K), and uric acid were entrusted to BML (Tokyo, Japan).

2-3 Renal morphology

The renal tissue was horizontally cut, after which half of the tissue was fixed in Carnoy's solution for 2 h, which was later changed to 70% alcohol overnight, for processing of the paraffin embedding. Sections of 5-μm thickness were prepared and separate sections were stained in hematoxylin and eosin (HE), periodic acid-Schiff (PAS), or Masson's trichrome staining (MTS). Semi-quantitative scoring for tubular vacuolation, glomerulosclerosis, and fibrosis was performed in a blinded fashion, according to the Banff 2018 classification[45]. In addition, the glomerulosclerosis and interstitial fibrosis were assessed using a Keyence BZ-x700 microscope (20×; Keyence, Osaka, Japan) with a 0.75 aperture. For interstitial fibrosis, the MTS-positive area (blue) was measured in

photomicrographs, at 20× magnification. Fibrotic area was quantified from three randomly selected cortex areas on each slide and determined by calculating the percentage of color-pixel count using the BZ-x Analyzer software (Keyence). To assess glomerulosclerosis, mesangial area was quantified from 10 randomly selected glomeruli per animal, using Image Pro Plus 6.0 software in PAS-stained tissues (40× magnification). The data were then exported into Excel (Microsoft, Washington, USA) to calculate the percentage of mesangial area per glomerulus area.

2-4 Western blot analyses

Rat kidney tissues were collected and lysed on ice using lysis buffer (T-PER; Pierce Biotechnology, Rockford, IL, USA) containing protease and phosphatase inhibitors. The lysates (500 μg) were denatured at 95 °C for 5 min in sample buffer, separated by means of sodium dodecyl sulfate-polyacrylamide gel electrophoresis (SDS–PAGE) on 10% gels, and electrophoretically transferred to polyvinylidene fluoride (PVDF) membranes. Nonspecific binding sites were blocked at room temperature with 5% bovine serum albumin in Tris-HCl buffer containing 0.1% Tween 20, for 2 h. The membranes were incubated with a primary anti-TGF-β antibody (catalog number: 3711; Cell Signaling Technology, Tokyo, Japan) and primary anti-glyceraldehyde-3-phosphate dehydrogenase (GAPDH) antibody (catalog number: 2118; Cell Signaling Technology), overnight

at 4 °C. Finally, the membranes were incubated with a horseradish peroxidase (HRP)-conjugated anti-rabbit IgG antibody (catalog number: 7074; Cell Signaling Technology) for 1 h. An enhanced chemiluminescence reagent (Nacalai Tesque, Kyoto, Japan) was used to detect the bound antibodies. The specific protein bands were detected using an LAS 4000 Mini Luminescent Image Analyzer (Cytiva, Marlborough, MA, USA). Densitometry data were normalized based on the amount of GAPDH in each sample.

2-5 Immunohistochemistry

Immunohistochemistry was performed on 5-μm-thick Carnoy's solution-fixed paraffin-embedded renal tissue sections using a primary anti-α-smooth muscle actin (α-SMA) antibody (catalog number: ab5694; Abcam, Cambridge MA, USA), anti-KIM-1 antibody (catalog number: AF3689; R&D Systems, Minneapolis, MN, USA), and anti-monocyte chemotactic protein 1 (MCP-1) antibody (catalog number: ab25124; Abcam) with a Dako EnVision™ detection kit (DakoCytomation, Carpinteria, CA, USA). Briefly, the slides were dried overnight at 65°C, de-paraffinized in xylene, and dehydrated using a series of graded alcohols. Non-specific binding sites were blocked by incubation with 3% skim milk in phosphate-buffered saline (PBS) for 10 min. The sections were then incubated with the primary antibody in a humid chamber, overnight at 4°C. Next, the slides were washed with PBS and endogenous peroxidase activity was inhibited by incubating the sections in 0.3% H_2O_2, for 30 min at room temperature.

The slides were then washed with PBS and incubated with a secondary antibody (catalog number: K4003, Dako EnVision™/HRP) for approximately 30 min at room temperature. DAB (catalog number: K5007, Dako EnVision™) was applied for approximately 2 min and then removed by rinsing with distilled water, following which the slides were then counterstained with hematoxylin. All sections were assessed and graded using a Keyence BZ-x700 microscope (20×), with a 0.75 aperture and processed using the BZ-x Analyzer software.

2-6 Statistical analysis

Data have been presented as mean ± SD. Multiple comparisons between groups were performed using one-way analysis of variance (ANOVA) with the Bonferroni *post-hoc* test, using Prism version 5.0 (GraphPad Software Inc., La Jolla, CA, USA). Statistical significance was set at $P < 0.05$.

3. Results

3-1 Body weight, renal function, and kidney/body weight

We first investigated the effect of TAC on body weight and renal function. No significant differences in initial body weight were observed between the groups. The post-body weight of the TAC+I/R group was markedly lower than that of the sham group ($P<0.05$). The TAC+I/R group, which received TAC daily for two weeks, had significantly lower renal function and higher levels of Scr, and BUN, as compared to those in the other groups. Table 2 shows the individual animal results for Scr and BUN levels in the TAC+I/R group. Serum Mg and K levels were significantly higher in the TAC+I/R group, as compared to those in the sham, IRI, and TAC groups, while serum uric acid levels were significantly lower in the TAC+I/R group. The relative kidney weight (kidney/body weight) was significantly lower in the sham and TAC groups, than those in the I/R and TAC+I/R groups.

Table 1. Basic parameter

	Sham (n=7)	I/R (n=7)	TAC (n=9)	TAC + I/R (n=7)
Pre-BW (g)	250.6 ± 9.0	243.5 ± 38.2	265.1 ± 14.4	272.9 ± 15.0
Post-BW (g)	294.6 ± 9.0	249.3 ± 25.5[a]	258.9 ± 17.9	237.8 ± 43.2[a]
BUN (mg/dL)	17.2 ± 1.2	22.8 ± 5.0	26.0 ± 7.5	168.3 ± 102.3[a,b,c]
Scr (mg/dL)	0.40 ± 0.07	0.26 ± 0.15	0.28 ± 0.02	4.02 ± 3.71[a,b,c]
Serum Mg (mg/dL)	2.37 ± 0.22	2.16 ± 0.11	1.67 ± 0.25	3.73 ± 0.96[a,b,c]
Serum K (mEq/L)	4.87 ± 0.55	5.44 ± 0.36	5.30 ± 0.82	8.80 ± 2.24[a,b,c]
Uric acid (mg/dL)	1.52 ± 0.74	1.53 ± 0.39	1.42 ± 0.40	0.64 ± 0.16[a,b,c]
K/B (Left kidney)	0.33 ± 0.02	0.40 ± 0.04[a, c]	0.32 ± 0.02	0.40 ± 0.04[a, c]
K/B (Right kidney)	0.34 ± 0.02	0.39 ± 0.05[a, c]	0.32 ± 0.04	0.39 ± 0.03[a, c]

BW, body weight; BUN, blood urea nitrogen; I/R, ischemia reperfusion; Scr, serum creatinine; TAC, tacrolimus; K/B, kidney/body weight. Values are expressed as mean ± SD.

[a]$p < 0.05$ vs. Sham; [b]$p < 0.05$ vs. I/R; [c]$p < 0.05$ vs. TAC; [d]$p < 0.05$ vs. TAC +I/R

Table 2. Individual animals result of TAC + I/R group

	Low dose TAC (2.5mg/kg) + I/R (n=10)		TAC (5.0mg/kg) + I/R (n=7)	
	BUN (mg/dl)	Scr (mg/dL)	BUN (mg/dl)	Scr (mg/dL)
1	38.1	0.30	256.72	3.75
2	35.2	0.36	246.79	5.03
3	35.8	0.32	38.34	0.61
4	43.4	0.31	252.14	10.06
5	39.0	0.35	75.83	0.93
6	35.4	0.30	243.28	7.33
7	25.1	0.21	64.66	0.40
8	39.1	0.34		
9	35.2	0.29		
10	37.4	0.35		
Mean±SD	36.37±4.7	0.31±0.04	168.25±102.31	4.02±3.71

BUN, blood urea nitrogen; I/R, ischemia reperfusion; Scr, serum creatinine; TAC, tacrolimus.

3-2 Morphological evaluation of renal tissue (HE and PAS staining)

Morphological changes in renal injury were investigated using HE and PAS staining. As shown in Figure 2A, HE and PAS staining of the renal tissue at 14 d post-reperfusion revealed tubular vacuolization and glomerulosclerosis in the TAC+I/R group, while no morphological changes were observed in the sham, IRI, and TAC groups. All of the animals in the TAC+I/R group had a vacuolization score of 3, which was significantly higher than that of the TAC group (score 0) which did not undergo I/R injury, and was treated with the same TAC dose. Fractional mesangial area was evaluated as the percentage of mesangial area per glomerulus area. The TAC+I/R group showed an increase in mesangial area, compared to that in the other groups (Figure 2B).

(A)

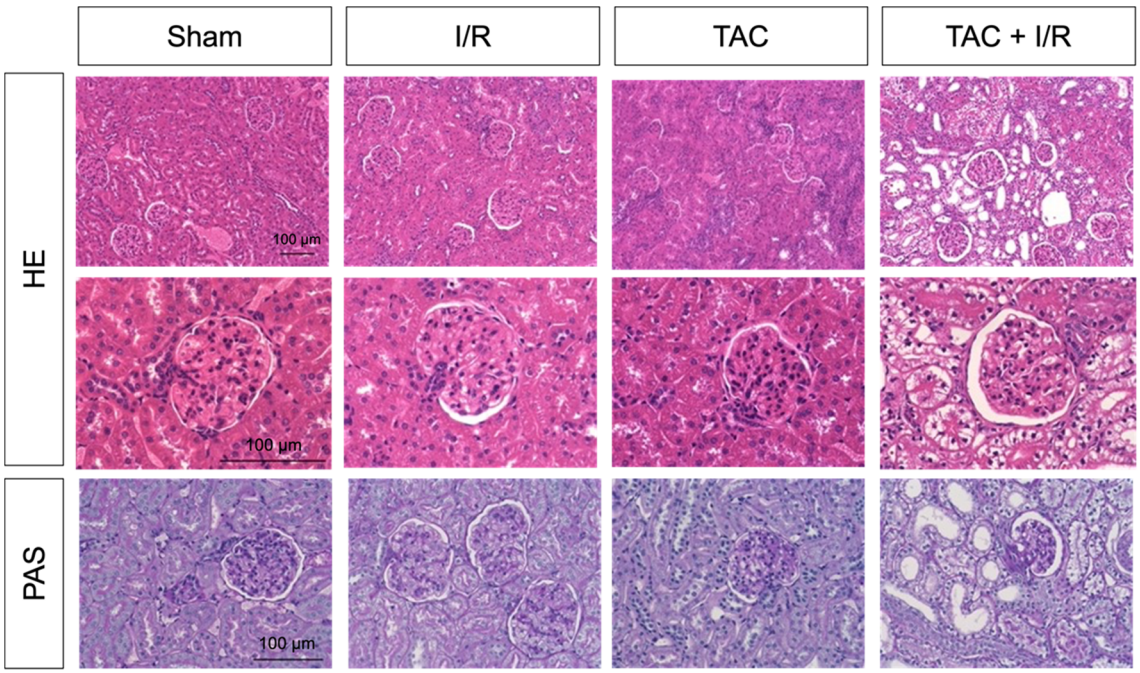

(B)

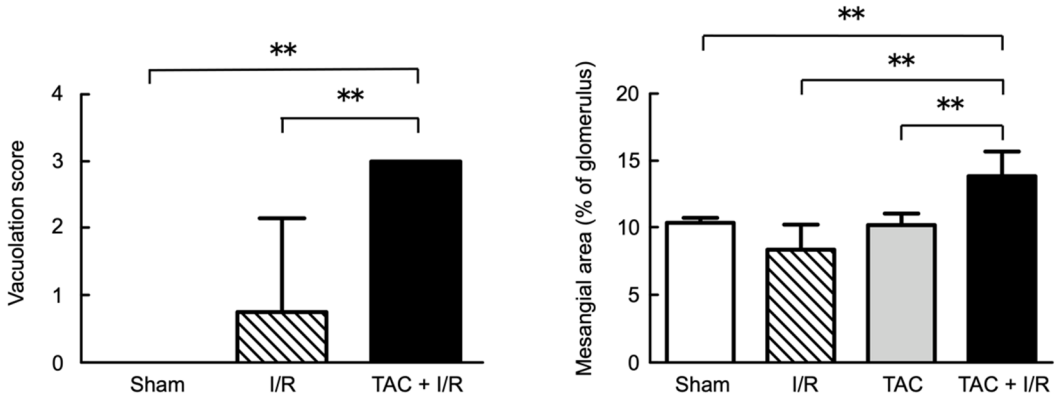

Figure 2. Tacrolimus-induced histopathological changes.

(A) Tubular vacuolization and glomerulosclerosis were observed in the TAC + I/R group following HE (×20 and x60) and PAS staining (×40). Scale bar = 100 μm. HE, hematoxylin and eosin staining; PAS, periodic acid-Schiff staining. (B) Quantitation of mesangial fractional volume for each group. Data are expressed as mean ± SD (**P < 0.01).

I/R, ischemia reperfusion; TAC, tacrolimus.

3-3 Evaluation of renal fibrosis

To evaluate the effect of TAC on renal fibrosis, we examined renal fibrosis using MTS and α-SMA staining (Figure 3A-3B). An MTS-positive signal (blue) represents collagen deposition and was considered as an indicator of fibrosis. The sham and TAC groups did not show any obvious MTS-positive cells, while the TAC+I/R group showed a significantly increased number of MTS-positive cells in the renal tubule-interstitium, as compared to that in the I/R group ($P<0.001$). In order to further investigate interstitial fibrosis caused by TAC, immunohistochemical analysis of α-SMA was performed, which is commonly used to assess the degree of renal fibrosis. As shown in Figure 3B, quantitative image analysis of α-SMA expression showed the same results as the MTS staining. No α-SMA expression was observed in the sham, I/R, and TAC groups. However, the TAC+I/R group showed high α-SMA expression in the renal tubule-interstitium ($P<0.001$). In addition, western blot analysis showed relatively low-level TGF-β protein expression in the sham, I/R, and TAC groups, while TGF-β protein levels were significantly higher in the TAC+I/R group (Figure 3C, $P<0.05$). No differences were observed between the sham, I/R, and TAC groups.

(A)

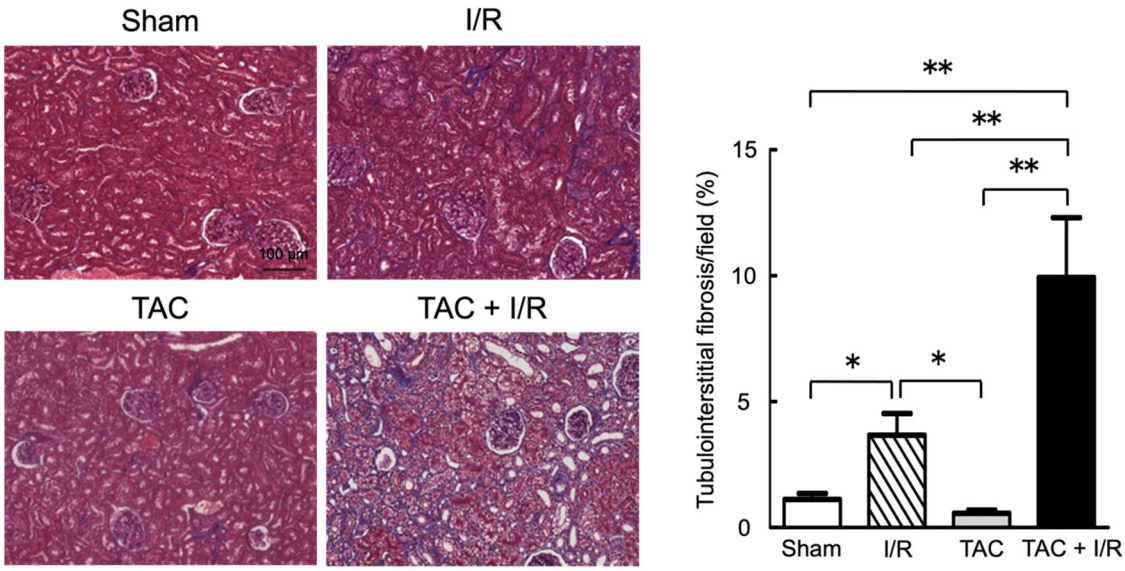
Sham
I/R
TAC
TAC + I/R
100 μm
Tubulointerstitial fibrosis/field (%)
15
10
5
0
*
*
**
**
**
Sham
I/R
TAC
TAC + I/R

(B)

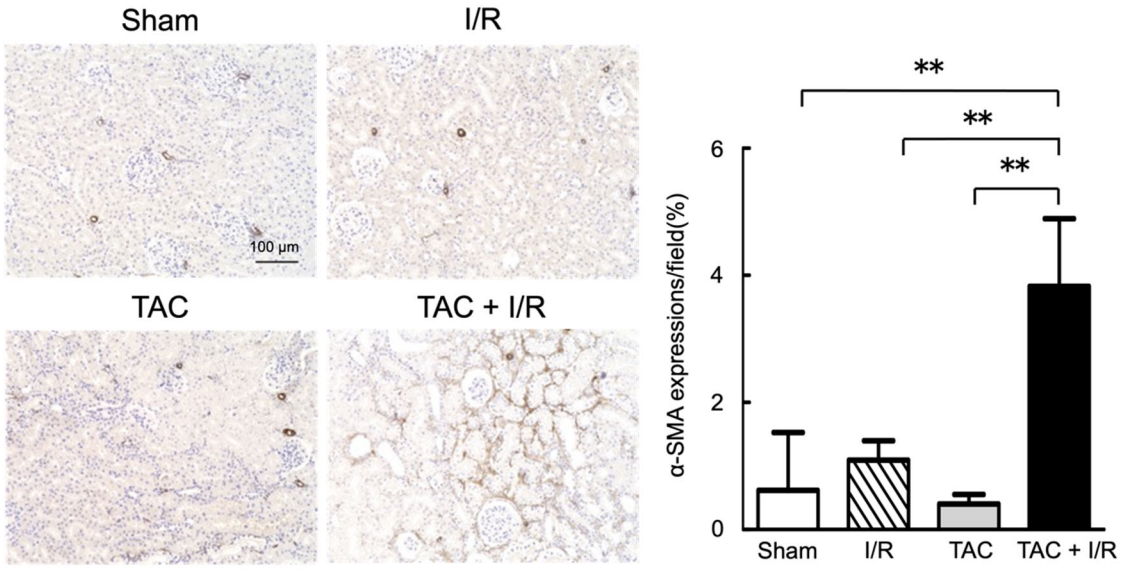
Sham
I/R
TAC
TAC + I/R
100 μm
α-SMA expressions/field(%)
6
4
2
0
**
**
**
Sham
I/R
TAC
TAC + I/R

(C)

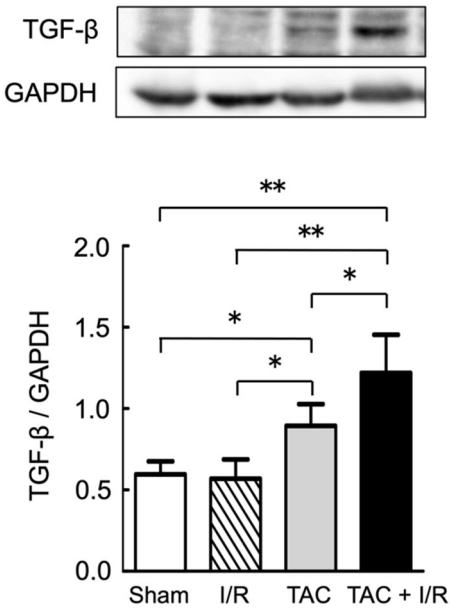

Figure 3. Tacrolimus-induced kidney interstitial fibrosis.

(A) Tubulointerstitial fibrosis was detected by MTS sections (×20). (B) Immunohistochemistry analysis of α-SMA expression level (×20). (C) Western blot demonstrating that tacrolimus increased TGF-β protein expression. Mean ± SD, n = 30. Scale bar = 100 μm, *P < 0.05, **P < 0.001. I/R, ischemia reperfusion; MTS, Masson's trichrome staining; α-SMA, α-smooth muscle actin; TAC, tacrolimus; TGF-β, transforming growth factor-β.

3-4 Evaluation of renal injury marker expression in the renal tissue

Next, we investigated the expression levels of several kidney injury markers including KIM-1 and MCP-1. There were significant differences in KIM-1 expression levels between the sham, I/R, and TAC groups; however, the TAC + I/R group exhibited significantly higher KIM-1 expression, as compared to that in the other groups ($P<0.001$), indicating TAC-induced nephrotoxicity (Figure 4A). In addition, proximal tubules in medullary rays also showed KIM-1 expression in the TAC+I/R group (Figure 4B), consistent with a previous report[46]. No significant difference in MCP-1 expression was observed between the three groups (Figure 5).

(A)

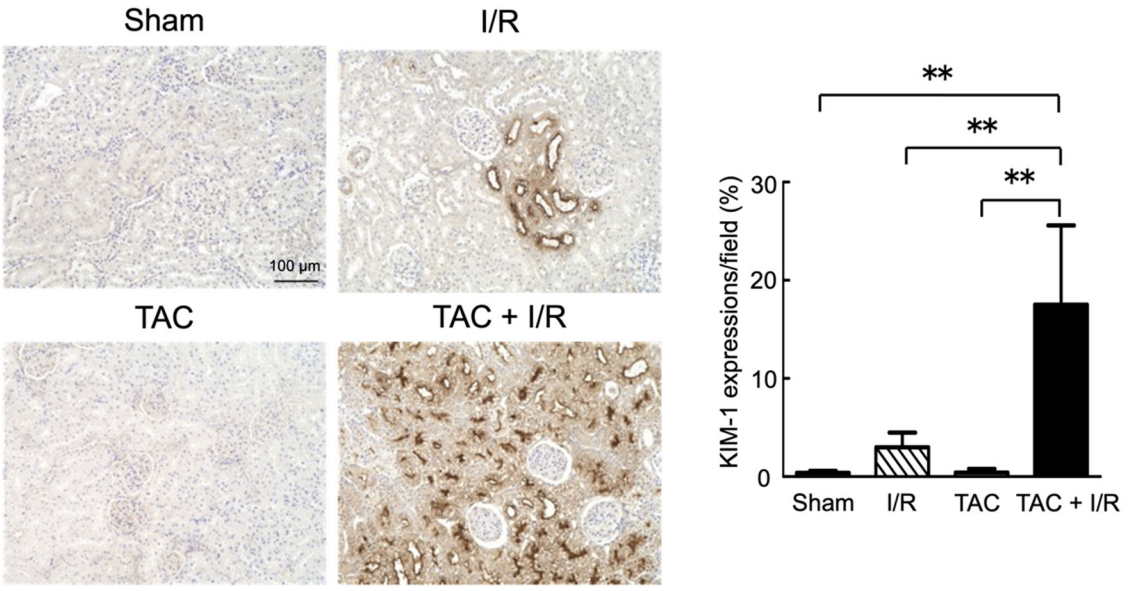

(B)

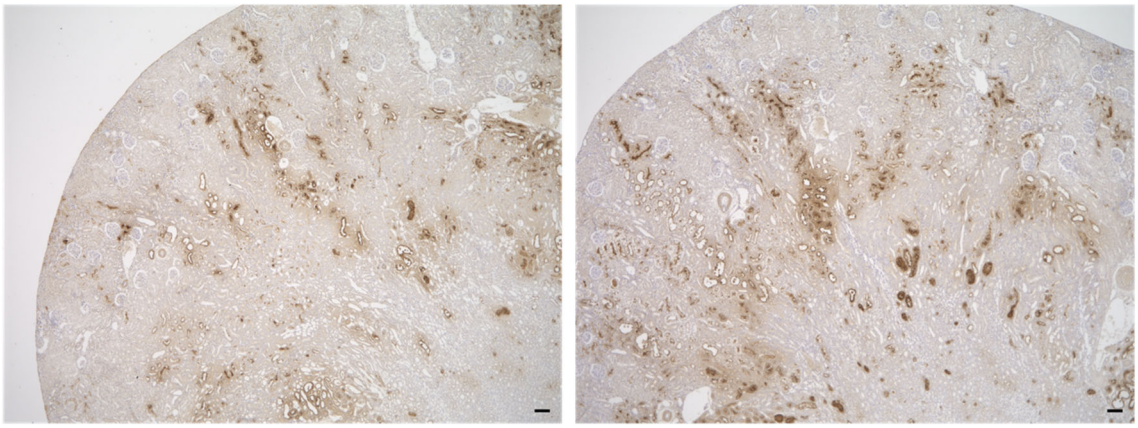

Figure 4. Tacrolimus-induced KIM-1 expression in kidney.

(A)Immunohistochemistry analysis of KIM-1 expression levels (×20). Semiquantitative scores of the percentage of stained area per high power filed for each group (mean ± SD, n = 30). (B) Immunohistochemistry analysis of KIM-1 expression levels (×4). Scale bar = 100 μm, **P < 0.001. I/R, ischemia reperfusion; TAC, tacrolimus; KIM-1, kidney injury molecule 1.

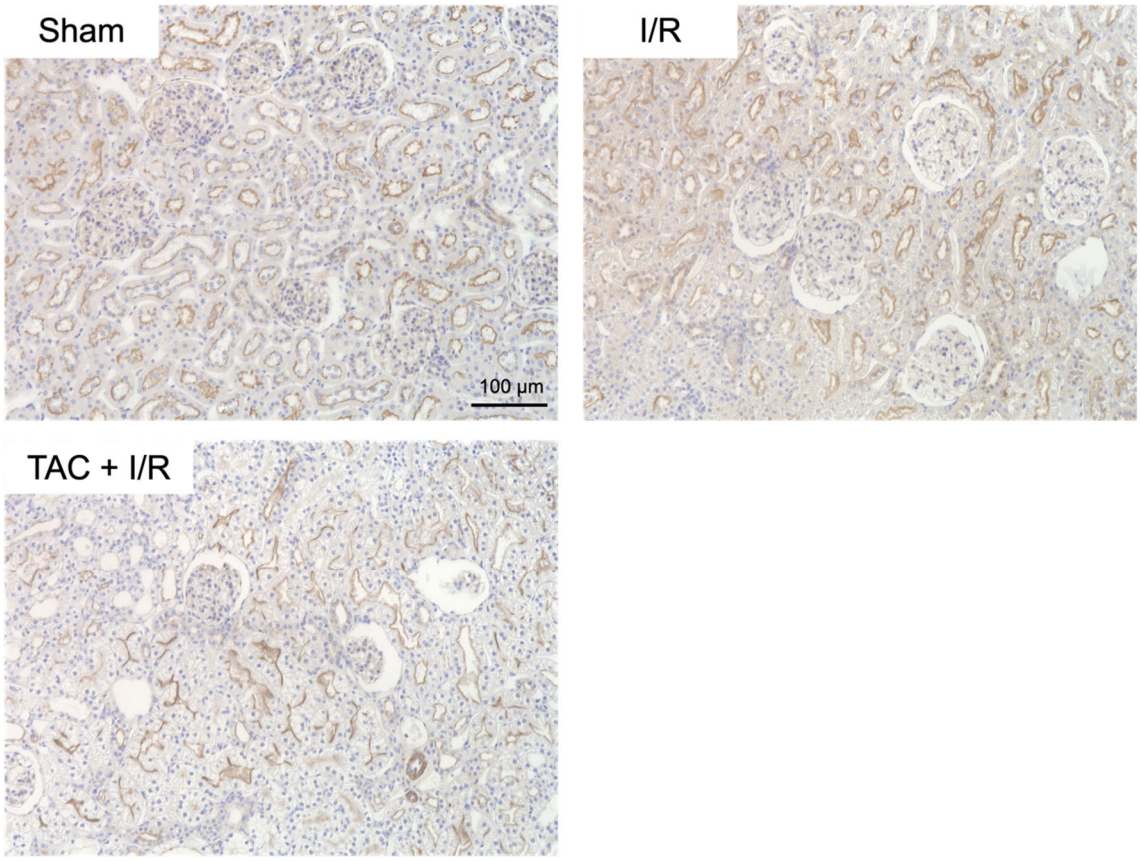

Figure 5. MCP-1 expression in kidney.

Immunohistochemical analysis of MCP-1 expression levels. Scale bar = 100 μm.

I/R, ischemia reperfusion; MCP-1, monocyte chemotactic protein 1; TAC, tacrolimus.

4. Discussion

In this study, we demonstrated the development of a TAC-induced nephropathy rat model with renal interstitial fibrosis using a new methodology consisting of 2-week TAC administration following renal ischemia reperfusion. In addition, we detected increased α-SMA, TGF-β, and KIM-1 expression in the renal tubulo-interstitium of these rats. Although several previous studies have reported TAC-induced nephropathy rat models, the development of a nephrotoxicity rat model *via* TAC monotherapy requires a three-month administration period[47]. A salt-depleted rat model, created to reduce the TAC administration period, exhibited renal injury-induced histological features similar to those in TAC-treated patients[43]. Salt depletion has been shown to accelerate the development of chronic TAC nephropathy, thereby shortening lesion development to four weeks[38, 48].

As renal fibrosis represents the common pathway of nearly all chronic and progressive human nephropathies[18], this study aimed to create a new TAC-induced nephrotoxicity rat model that would reduce the time required for renal fibrosis development. We performed I/R in Wistar rat kidneys and then subcutaneously administered TAC to the rats, at a dose of 5 mg/kg per day, for two weeks. Compared to the sham, I/R, and TAC groups, the TAC+I/R group showed decreased kidney function, as demonstrated by significantly increased Scr and BUN levels, which indicate damaged glomerular function, and increased

serum Mg and K as well as uric acid levels, which indicate damaged tubular dysfunction. HE and PAS staining revealed noticeable kidney injury, such as tubular vacuolization and glomerulosclerosis, in the TAC+I/R group.

The role of TGF-β in TAC-induced nephrotoxicity has been extensively studied. *In vivo* and *in vitro* experiments have shown that TAC enhances TGF-β expression *via* direct activation of the TGF-β promoter and mRNA synthesis, thereby causing excessive accumulation of the extracellular matrix, leading to fibrosis[49, 50]. Furthermore, TGF-β expression has been found to be high in renal transplant recipients diagnosed with TAC nephrotoxicity[51, 52]. Our results showed a significant increase in TGF-β expression, as well as increased MTS-positive cells and α-SMA expression in the TAC+ I/R group, as compared to those in the sham, IRI, and TAC groups, indicating that TAC induced interstitial fibrosis. KIM-1 is a type 1 transmembrane protein that cannot be detected in the normal kidney tissue and urine[53]. However, it is expressed at very high levels in the proximal tubules, shortly after kidney injury such as ischemic and toxic insults[54]. Among kidney transplantation patients, higher urine KIM-1 levels are independently and differentially associated with a greater risk of adverse outcomes[55]. Although KIM-1 is known as a sensitive biomarker of AKI, studies have also shown that sustained KIM-1 expression promotes kidney fibrosis, and high KIM-1 expression indicates kidney fibrosis[56, 57]. KIM-1 expression levels have been shown to be significantly high in both the tissue and urine of kidney transplantation patients with renal biopsy-confirmed kidney fibrosis[58]. MCP-1 is

also used as a urinary biomarker for cisplatin-induced AKI[59] and IgA nephropathy[60]; however, this study did not observe MCP-1 expression in the TAC+I/R group (Figure 5). Thus, our rat model possibly develops nephropathy *via* a process other than cisplatin and IgA nephropathy.

Our data showed that both TAC and I/R injury are indeed nephrotoxic, but TAC or I/R injury alone may not be nephrotoxic. These data also show that I/R injury contributes significantly to the development of TAC-induced nephrotoxicity. The role of increased TGF-β expression in TAC and I/R injury has to be evaluated in connection with the cumulative nephrotoxicity of I/R injury and TAC treatment. While the increased expression of TGF-β may represent a physiologic adaptation to I/R injury, its persistence may indicate irreversible renal damage. In addition, the injury caused by I/R is inevitable in renal transplant recipients and several studies have already shown that I/R-induced AKI can lead to renal fibrosis and is an important risk factor for CKD[61, 62]. Thus, a possible mechanism is that after I/R injury, the defects in the progression of the cell cycle may switch tubular cells to a pro-fibrotic phenotype, and along with the subsequent damage from TAC, the cell may continue produce pro-fibrogenic growth factors that stimulate fibroblast proliferation and collagen production, thereby accelerating TAC-induced fibrosis in rats. Similarly, our study shows that although there was no significant decrease in kidney function in the IRI group, as compared to that in the sham group, it could serve as a sensitive indicator of possible existing kidney injury[63]. The relative kidney weight (both

left and right kidney) was significantly lower in the sham and TAC groups, as compared to those in the IRI and TAC+I/R groups; in addition, subsequent fibrosis analysis indicated the potential existence of kidney damage caused by I/R. We administered TAC subcutaneously because according to a previous report, oral administration has a much lower bioavailability[38]. Although the daily tacrolimus dose (5 mg/kg) used in the present study is high based on weight, it is still feasible since TAC has a higher clearance and larger distribution volume in rats, as compared to those in humans[64]. To suppress renal allograft rejection in rats, the most effective dose of TAC tested was 3.2 mg/kg per day, which is higher than the dose in clinical use for kidney transplant patients[65]. In addition, experimental studies have reported that when rats were orally administered TAC at a daily dose of 5 mg/kg for 4 weeks, there was no elevation in BUN and Scr levels[66]. We also performed experiments with renal I/R injury on day 1 and treatment with low dose TAC (2.5mg/kg/day) for two weeks (low dose TAC+I/R), but observed that the BUN and Scr levels were not elevated (Table 2). Thus, it was suggested that the optimal dose of TAC in an experimental model combining TAC-induced nephrotoxicity and I/R injury was subcutaneous administration at a dose of 5 mg/kg, daily for two weeks.

5. Conclusions

In summary, we report a new method for developing TAC-induced nephropathy with renal interstitial fibrosis in a short time. In addition, we found that α-SMA, TGF-β, and KIM-1 were expressed in the kidneys of these TAC-induced nephropathy rats. We hope that this model will help elucidate the mechanism underlying TAC-induced nephropathy in future studies.

Chapter 2. The hypoxia-inducible factors prolyl hydroxylase inhibitor roxadustat attenuates tacrolimus-induced renal interstitial fibrosis in rats

1. Introduction

In the previous study, we established a rat model of TAC-induced nephrotoxicity and proposed the hypothesis that I/R injury accelerates TAC-induced nephrotoxicity.

After I/R-induced acute kidney injury, the kidneys have the capability to repair damaged tubules. Depending on the severity of injury, the repair can be complete or incomplete. Complete repair (also called "adaptive repair") can restore the integrity and function of renal tubules, whereas incomplete or maladaptive repair, characterized by undifferentiated and atrophic tubules and persistent inflammation, leads to renal interstitial fibrosis. Tubulointerstitial hypoxia is considered to be a common pathway for progressive kidney disease[67]. Tubular epithelial cells are rendered particularly prone to hypoxic injury due to their high metabolic activity and large oxygen demand. After I/R injury, the epithelial cells initiate inflammatory response by recruiting inflammatory cells to the injured interstitium and secreting a variety of fibrogenic cytokines and inflammatory factors, such as platelet-derived growth factor, fibroblast growth factor-2, tumor necrosis factor-1α, and IL-6, which subsequently activate

fibroblasts and tubular epithelial cells. In addition, the epithelial cells are stimulated to undergo apoptosis, cell cycle arrest, and phenotypic transition as well as epithelial-to-mesenchymal (EMT) transition *via* loss of their epithelial feature and acquisition of the mesenchymal phenotype, thereby contributing to tubular atrophy and accumulation of extracellular matrix proteins. Eventually, the excess deposition of extracellular matrix proteins in the interstitium extends the distance between capillaries and nearby nephrons, and leads to endothelial dysfunction and peritubular microvascular rarefaction, which, in turn, aggravats hypoxia, forming a vicious circle. Together, these fibrogenic events conjunctly result in tissue destruction, eventually leading to kidney fibrosis[68-77]. In conclusion, hypoxia can convert tubular epithelial cells to a pro-fibrotic phenotype and promote tubulointerstitial inflammation; maladaptive repair post-I/R leads to renal interstitial fibrosis. Increasing evidence indicates that HIF is a pivotal regulator of kidney fibrosis under various pathological conditions.

ROX is an oral HIF-PHD inhibitor, that can stabilize HIF and increase iron utilization, thereby stimulating erythropoietin production, and is thus used as a novel treatment for anemia of CKD[78]. Some studies have shown that ROX ameliorated AKI-induced kidney injury caused by I/R. Pretreatment with ROX significantly ameliorated kidney function and kidney histological damage in mice after I/R injury, by reducing tubular cells apoptosis, attenuating mitochondrial damage, and alleviating DNA damage after I/R injury[79]. In another study, ROX was shown to protect against I/R-induced kidney injury, by

diminishing tubular cell injuries and suppressing sequence inflammatory responses[80]. In addition, the administration of ROX to mice at 3 d after unilateral kidney I/R markedly alleviated kidney fibrosis and enhanced renal vascular regeneration, thereby demonstrating the therapeutic effect of ROX in preventing the AKI-to-CKD transition related to ischemia[32]. ROX also alleviated AKI-induced kidney injury caused by other factors such as folic acid and cisplatin, *via* angiogenesis and activation of the Akt/GSK-3β/Nrf2 pathway[33, 81, 82]; however, the effects of ROX in TAC-induced nephropathy after I/R are unknown.

In the present study, we aimed to investigate the effect of ROX on the TAC-induced nephrotoxicity rat.

2. Materials and Methods

2-1 Animals and Drugs

Male Wistar rats weighing 250–270 g at 8–9 weeks of age purchased from SLC were housed under standard conditions with water and food ad libitum. Experiments were performed in accordance with the Guidelines for Animal Experiments of Kyushu University. All experimental protocols were approved by the Animal Research Committee of the Graduate School of Medicine, Kyushu University (approval number: A20-007-0).

The purchased rats were housed under controlled temperatures of 25 ± 1°C and 12h/12h light/dark cycle, with water and food *ad libitum*. Before drug administration, renal I/R injury was performed according to a previously published protocol[44]. Rats were anesthetized by means of isoflurane inhalation, with a 4% dose for induction and a 1.5% dose for maintenance. The abdominal cavity was then exposed using midline laparotomy. Subsequently, both renal pedicles were cross-clamped for 45 min. During ischemia, the rats were hydrated with saline and maintained at 37°C using heating plates. Renal clamps were removed after 45 min, and all incisions were closed. After surgery, the animals were placed on the heating plates until recovery from anesthesia, and then moved to cages with free access to water and standard rat chow.

The rats (n = 25) were randomly divided into four groups: (1) sham group,

sham operation on day 1 and treatment with saline and vehicle (n=8); (2) ROX group, sham operation on day 1 and treatment with saline and ROX (3 mg/kg per 2d, n=4); (3) TAC group, renal I/R injury on day 1 and treatment with TAC (5 mg/kg per day) and vehicle (n=6); (4) TAC+ROX group, renal I/R injury on day 1 and treatment with TAC (5 mg/kg per day) and ROX (3 mg/kg per 2d, n=7).

TAC (5 mg/kg; Prograf; Astellas Pharma Inc) was subcutaneously administered to the backs of the TAC and TAC+ROX groups, once daily for two weeks. For ROX (Cayman Pharma, Estonia, Czech Republic) administration, 50 mg of ROX was dissolved in 2 mL of dimethyl sulfoxide (DMSO) as a stock solution, which was subsequently diluted with PBS into working concentrations (5 mg/mL). ROX was gavage administered to the ROX and TAC+ROX groups, every two days, for 16 d. In addition, 0.24–0.26 mL of saline was subcutaneously administered to the sham and ROX groups, once daily for two weeks, while 0.14–0.16 mL of vehicle (20% DMSO in PBS) was gavage administered to the sham and TAC groups, every two days, for 16 d.

All rats were sacrificed on day 15. After the rats were anesthetized, their whole blood and serum samples were collected by means of cardiac puncture, following which their kidneys were harvested. The right kidney from each animal was cut into half. One-half of each kidney was snap-frozen in liquid nitrogen and subsequently stored at −80°C for use in western blott. The other half was fixed in Carnoy's solution for further analysis. Figure 6 shows a

schematic representation of the experimental procedure.

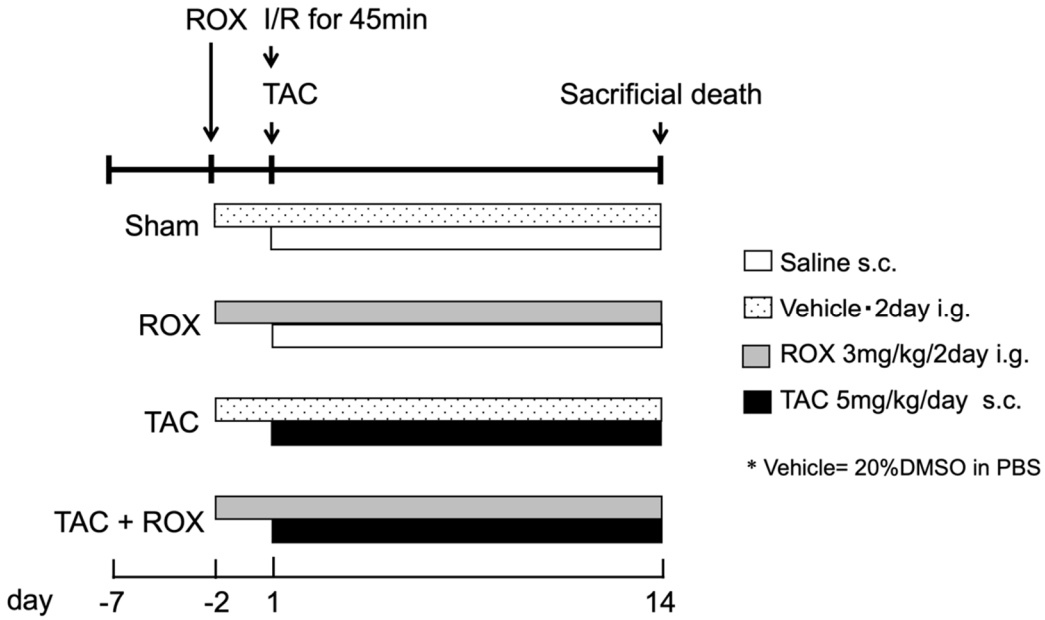

Figure 6. Schematic illustration of the experimental protocol.

Sham group, sham-operated in kidney and treated with saline for 14 d as well as with vehicle every 2 d, for 16 days; ROX group, bilateral kidney ischemia was induced at day 1 for 45 min and treated with saline for 14 d and with ROX(3 mg/kg/2d) for 16 d; TAC group, sham-operated in kidney and treated with tacrolimus (5 mg/kg/d) for 14 d; TAC+ROX group, bilateral kidney ischemia was induced at day 1 for 45 min and treated with tacrolimus (5 mg/kg/d) for 14 d and as well as ROX (3 mg/kg/2d) for 16 d. The rats were sacrificed under anesthesia on day 15, following which their blood samples and tissue specimens were obtained for further analyses.

i.g., intragastrical administration; I/R, ischemia reperfusion injury; ROX, roxadustat; s.c., subcutaneous administration; TAC, tacrolimus.

2-2 Evaluation of renal function

Rat whole blood was centrifuged for 10 min at 3000 rpm following which the upper serum was collected and stored at −80°C until further use. Concentrations of Scr, BUN, uric acid, as well as serum K and Mg levels were measured by BML, to assess renal function.

2-3 Renal morphology

The renal tissue was horizontally cut, and half of the tissue was fixed in Carnoy's solution for 2 h, following which it was changed into 70% alcohol overnight, for processing of the paraffin embedding. Sections of 5-μm thickness were prepared and separate sections were stained in HE, PAS, or MTS. The glomerulosclerosis and interstitial fibrosis were assessed using a Keyence BZ-x700 microscope (20×) with a 0.75 aperture. For interstitial fibrosis, the MTS-positive area (blue) was measured in photomicrographs, at 20× magnification. Fibrotic area were quantified in five randomly selected cortex areas on each slide and determined by calculating the percentage of color-pixel count using the BZ-x Analyzer software. To assess glomerulosclerosis, mesangial area was quantified from 10 randomly selected glomeruli per animal, using Image Pro Plus 6.0 software, in PAS-stained tissues (40× magnification). The data were then exported into Microsoft Excel, to calculate the percentage of mesangial area per glomerulus area.

2-4 Immunohistochemistry

Immunohistochemistry was performed on 5-μm-thick Carnoy's solution-fixed paraffin-embedded renal tissue sections, using a primary anti-KIM-1 antibody (catalog number: AF3689; R&D Systems) and anti-F4/80 antibody (catalog number: PA5-21399, Thermo Fisher Scientific, Waltham, MA, USA) with a Dako EnVision™ detection kit (DakoCytomation). Briefly, the slides were dried overnight at 65°C, deparaffinized in xylene, and dehydrated using a series of graded alcohols. Non-specific binding sites were blocked by means of incubation with 3% skim milk in PBS for 10 min. The sections were then incubated with the primary antibody in a humid chamber, overnight at 4°C. Next, the slides were washed with PBS and the endogenous peroxidase activity was inhibited by incubating the sections in 0.3% H_2O_2 for 30 min at room temperature. The slides were then washed in PBS and incubated with the secondary antibody (catalog number: K4003, Dako EnVision™/HRP) for approximately 30 min at room temperature. DAB (catalog number: K5007, Dako EnVision™) was applied for approximately 2 min and then removed by rinsing with distilled water, following which the slides were counterstained with hematoxylin. All sections were assessed and graded using a Keyence BZ-x700 microscope (20×) with a 0.75 aperture and processed using the BZ-x Analyzer software.

2-5 Statistical analysis

Data has been presented as mean ± SD. Multiple comparisons between groups were performed using one-way ANOVA with the Bonferroni's *post-hoc* test, on the software Prism version 5.0 (GraphPad Software Inc). Statistical significance was set at $P<0.05$.

3. Results

3-1 TAC-induced kidney injury is attenuated upon ROX administration

At first, we evaluated the effects of ROX on renal function in the TAC-induced nephrotoxicity rat. No significant differences in initial body weight were observed between the groups. The post-body weight of the TAC and TAC+ROX groups were markedly lower than those of the sham and ROX groups ($P<0.05$). After 2 weeks of TAC administration, there was a significant elevation of Scr, BUN, as well as serum Mg and K levels, in addition to both right and left kidney/body weight and general kidney function markers (Table 3). Increased expression of KIM-1, a marker protein for tubular injury, was also observed upon immunohistochemical staining (Figure 7). ROX co-administration with TAC significantly reduced Scr (Table 3) and KIM-1expression (Figure 7). It must be noted that we did not find obvious side effects of ROX treatment on the renal function in rat.

Table 3. Basic parameter

	Sham (n=8)	ROX (n=4)	TAC (n=6)	TAC+ROX (n=7)
Pre-BW (g)	250.6 ± 9.0	245.8 ± 3.3	254.9 ± 7.9	249.4 ± 6.7
Post-BW (g)	285.5 ± 13.0	286.2 ± 6.2	204.2 ± 30.4[a,b]	235.6 ± 29.2[a,b]
BUN (mg/dL)	19.3 ± 1.55	18.0 ± 1.45	236.6 ± 172.8[a,b]	99.7 ± 88.4
Scr (mg/dL)	0.25 ± 0.02	0.28 ± 0.03	2.5 ± 3.0[a,b,d]	0.74 ± 0.45
Serum Mg (mg/dL)	2.05 ± 0.21	2.20 ± 0.16	3.45 ± 1.27[a]	2.29 ± 0.97
Serum K (mEq/L)	5.06 ± 0.81	5.78 ± 1.04	6.82 ± 1.6[a]	5.79 ± 0.88
Uric acid (mg/dL)	0.81 ± 0.34	0.98 ± 0.13	0.53 ± 0.18	0.63 ± 0.17
K/B (Left kidney)	0.31 ± 0.02	0.33 ± 0.03	0.46 ± 0.07[a,b]	0.48 ± 0.07[a,b]
K/B (Right kidney)	0.33 ± 0.03	0.33 ± 0.01	0.42 ± 0.05[a,b]	0.45 ± 0.05[a,b]

BW, body weight; BUN, blood urea nitrogen; ROX, roxadustat; Scr, serum creatinine; TAC, tacrolimus; K/B, kidney/body weight. Values are expressed as mean ± SD.

[a]$p < 0.05$ vs. Sham; [b]$p < 0.05$ vs. ROX; [c]$p < 0.05$ vs. TAC; [d]$p < 0.05$ vs. TAC + ROX

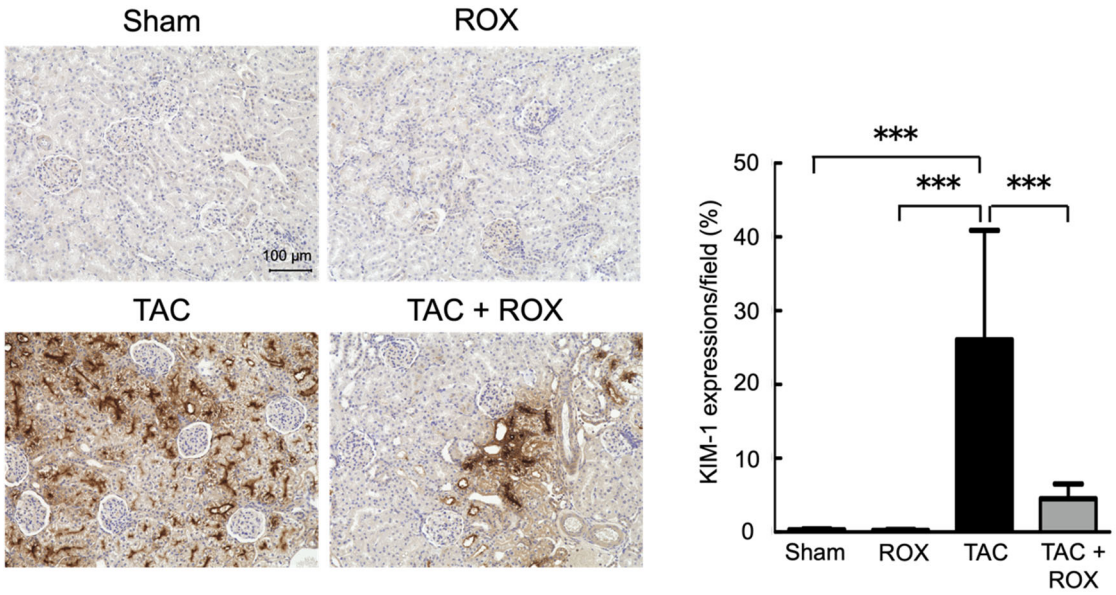

Figure 7. Tacrolimus-induced KIM-1 expression.

Immunohistochemistry analysis of KIM-1 expression levels (×20). Semiquantitative scores of the percentage of stained area per high power filed for each group (mean ± SD, n = 25). Scale bar = 100 μm, ***P < 0.001.

ROX, roxadustat; TAC, tacrolimus; KIM-1, kidney injury molecule 1.

3-2 TAC-induced glomerulosclerosis is attenuated upon ROX administration

Morphological changes in renal injury were investigated using HE and PAS staining. As shown in Figure 8A, HE and PAS staining of the renal tissue at 14 days post-reperfusion revealed dilated tubules; in addition, tubular vacuolization was observed in the kidneys of rats administered TAC alone. Remarkably, these histological changes were alleviated after treatment with ROX (Figure 8A).

To examine the effects of ROX on mesangial matrix expansion in TAC-induced nephrotoxicity rat, we assessed mesangial matrix expansion by means of PAS staining in the four groups of rats. Fractional mesangial area was evaluated as the percentage of mesangial area per glomerular area. The TAC group showed significantly decreased glomerular area, and increased degree of mesangial matrix area and mesangial matrix expansion, as compared to those in the sham group (Figure 8B–8C). When we treated TAC-induced nephrotoxicity rat with ROX for 16 d, glomerular area, mesangial matrix area, and mesangial matrix expansion were significantly ameliorated (Figure 8B–8C). No obvious side effects of ROX treatment were found on glomerulosclerosis in rat (Figure 8A–8C).

(A)

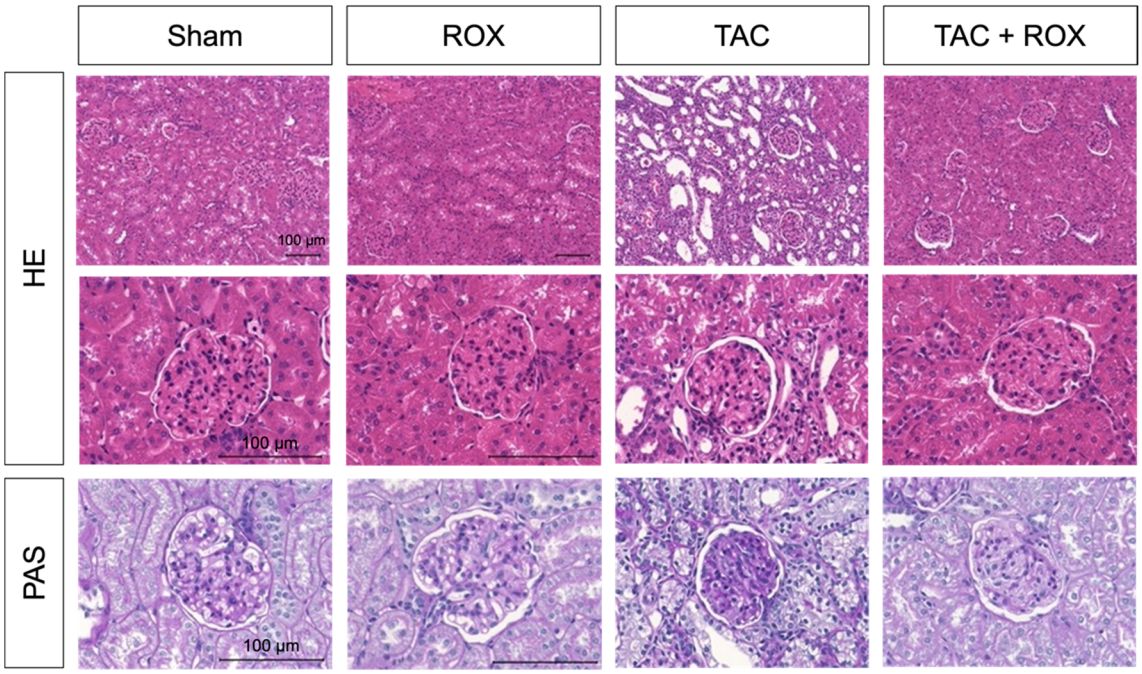
Sham
ROX
TAC
TAC + ROX
HE
PAS
100 μm
100 μm
100 μm

(B)

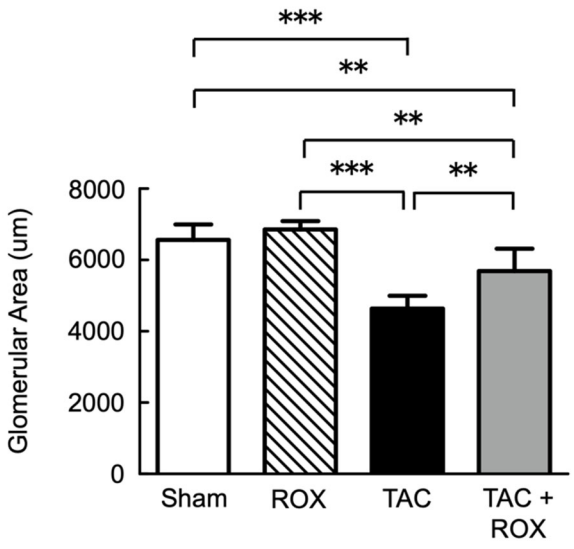
***
**
**
***
**
Glomerular Area (um)
8000
6000
4000
2000
0
Sham
ROX
TAC
TAC + ROX

(C)

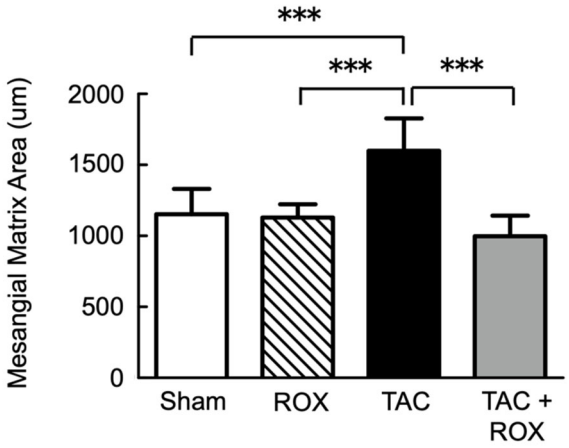

(D)

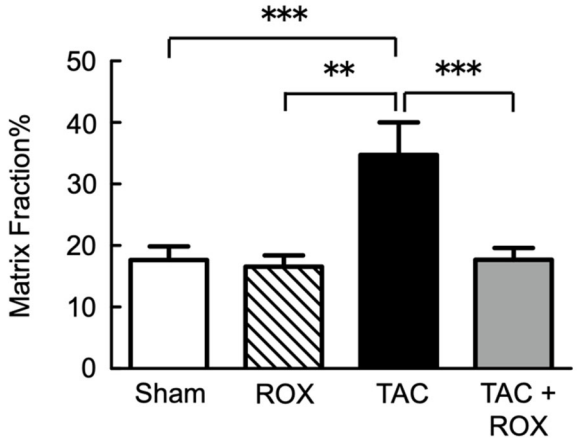

Figure 8. Tacrolimus-induced histopathological changes.

(A) Tubular vacuolization and glomerulosclerosis were observed in the TAC group following HE (×20 and x60) and PAS staining (×60). Scale bar = 100 μm. HE, hematoxylin and eosin staining; PAS, periodic acid-Schiff staining. (B) Quantitation of glomerular area for each group. (C) Quantitation of mesangial matrix area for each group. (D) Quantitation of matrix fraction for each group. Data are expressed as mean ± SD (**P < 0.01, ***P < 0.001).

ROX, roxadustat; TAC, tacrolimus.

3-3 TAC-induced renal fibrosis is attenuated upon ROX administration

To evaluate the effect of ROX on renal fibrosis in TAC-induced nephrotoxicity rat, we examined renal fibrosis using MTS staining (Figure 9). An MTS-positive signal (blue) represents collagen deposition and was considered as an indicator of fibrosis. The sham and ROX groups did not show any obvious MTS-positive cells, while the TAC group showed a significantly increased number of MTS-positive cells in renal tubule-interstitium fibrosis, as compared to those in the sham and ROX groups ($P<0.001$). After ROXco-administration with TAC for 16 d, there was a significant reduction in the renal tubulo-interstitium fibrosis (Figure 9). No differences were observed between the sham, ROX and TAC+ROX groups.

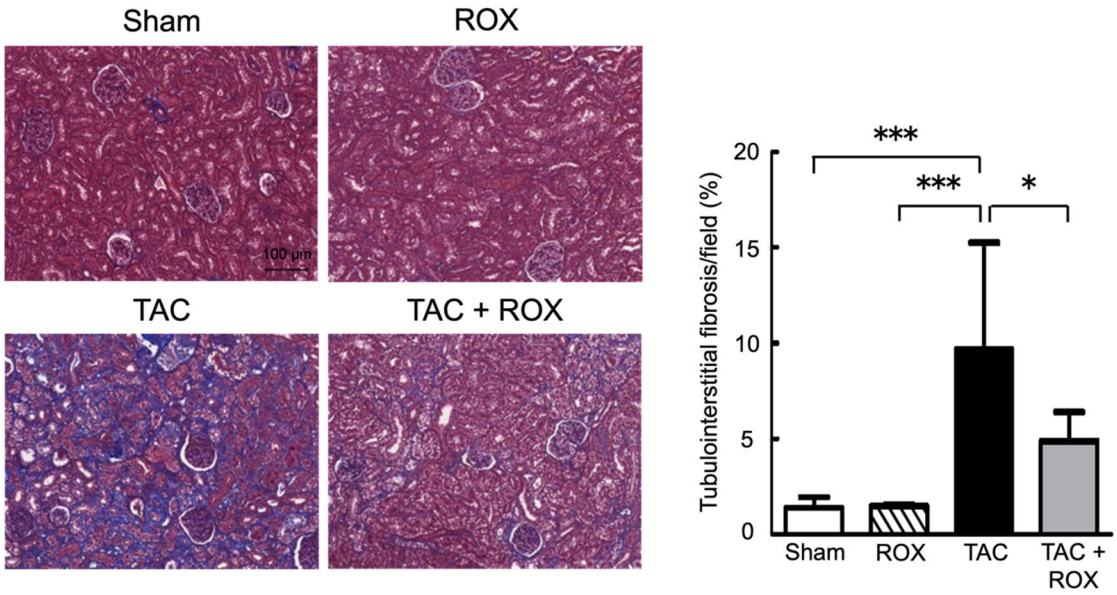

Figure 9. Tacrolimus-induced kidney fibrosis.

Tubulointerstitial fibrosis was detected by MTS sections (×20). MTS, Masson's trichrome staining.

Scale bar = 100 μm. Data are expressed as mean ± SD. (*P < 0.05, ***P < 0.001)

ROX, roxadustat; TAC, tacrolimus.

3-4 ROX suppresses tacrolimus-induced macrophage infiltration in the kidney cortex

To characterize the effect of ROX on inflammation in TAC-induced nephrotoxicity rat, immunohistochemistry of F4/80, a macrophage marker, was conducted to assess macrophage infiltration. TAC single administration increased the positive F4/80 staining area, as compared to that in sham and ROX groups, while ROX co-administration significantly decreased F4/80 expression (Figure 10).

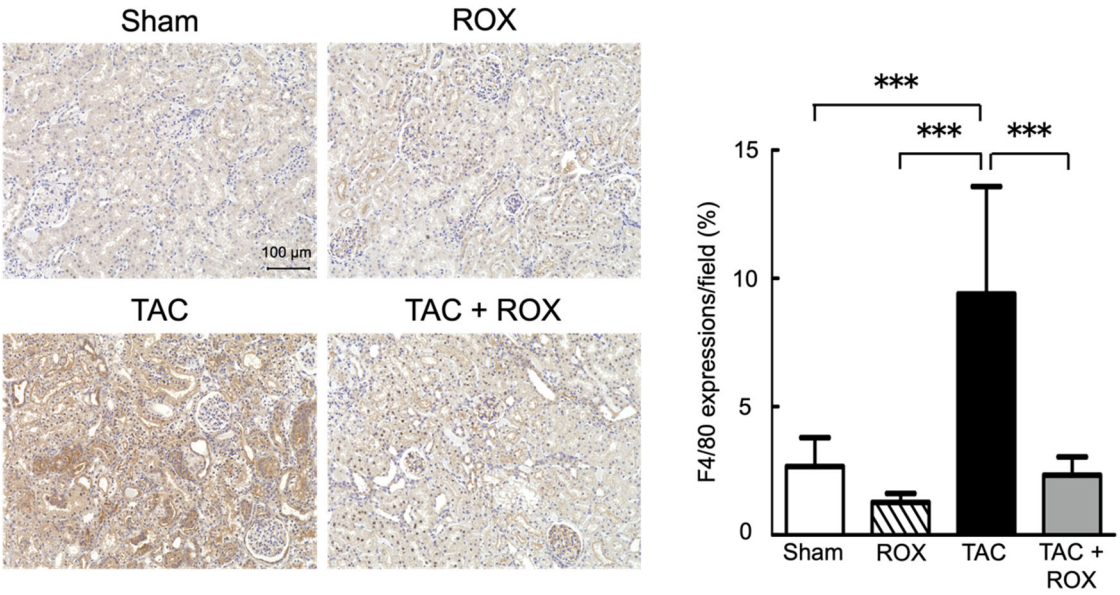

Figure 10. Tacrolimus-induced macrophage infiltration.

Immunohistochemistry analysis of F4/80 expression levels (×20). Semiquantitative scores of the percentage of stained area per high power filed for each group (mean ± SD, n = 25). Scale bar = 100 μm, ***P < 0.001.

ROX, roxadustat; TAC, tacrolimus.

4. Discussion

ROX is a novel HIF stabilizer that is currently applied for the treatment of renal anemia. In this present study, we explored whether ROX can protect against TAC-induced kidney injury, by inhibiting kidney fibrosis. Our results demonstrated that ROX remarkably ameliorated the TAC-induced kidney injury.

In the present study, ROX significantly ameliorated TAC caused tubule-interstitium fibrosis, glomerulosclerosis, and inflammation, thereby improving kidney function, as evidenced by reduced Scr levels and expression of KIM-1.

The exposure of rats to ROX at an oral dose of 10 mg/kg resulted in 4.5- to 3.6-fold higher AUC and 5.4- to 4.0-fold higher Cmax than those measured in a phase I clinical study in healthy subjects, using the anticipated clinical maximal doses of 2 and 3 mg/kg[83]. When such values were fitted to the doses used in the present study, a dose of 3 mg/kg corresponded to a 1.35- to 1.08-fold higher AUC and 1.62- to 1.2-fold higher Cmax observed at 2-3 mg/kg dose given orally to the healthy volunteers. Therefore, a dose of 3 mg/kg used in the present study is comparable to the maximal dose used in the clinical setting. Administration every two days will ensure low-frequency and stable HIF activation, thereby aiding the efficacy and reducing the side effects[84]. In addition, a previous study reported that the timing of using HIF-PHD inhibitor will influence the effect, and thus, ROX was given two days before I/R injury[85].

Numerous studies have shown that activation of HIF can inhibit AKI induced by various factors, such as I/R injury and cisplatin[82, 86-88]. However, there is controversy regarding the effect of HIF on fibrosis in experimental models of CKD. On the one hand, an inappropriate and prolonged activation of HIF is well known to play a pivotal role in initiating and promoting renal fibrogenesis *via* regulation of multiple signaling pathways in CKD. Mechanistically, HIF signaling may promote renal fibrosis *via* at least four mechanisms: (1) transcriptional regulation of fibrogenic genes; (2) cross-talk with other pro-fibrotic signaling pathways such as TGF-β, NF-κB, Notch, and PI3K/Akt pathways; (3) a potential role in EMT; and (4) epigenetic regulation[89]. On the other hand, activation of HIF could attenuate renal injury and fibrosis in the CKD rat model. Using the rat remnant kidney model to induce renal fibrosis, the pharmacological activation of HIF attenuated renal injury and tubulointerstitial fibrosis[26-29]. Another study showed that global activation of HIF repressed fibrogenesis in mice subjected to unilateral ureteral obstruction[30]. In addition, in the mouse model of cyclosporin A-induced toxicity, activated HIF improved renal function *via* the inhibition of apoptosis, inflammation and fibrosis[31].

We speculate that the possible reasons for the cause of significant discrepancy between these studies regarding the role of HIF in renal fibrosis are as follows: (1) activated isoforms are different. It is generally believed that the activation of HIF-1α contributes to the occurrence of fibrosis, while the activation of HIF-2α has an anti-fibrotic effect[90, 91]; (2) the dose of HIF-PHD inhibitor will

influence the effect of fibrosis. One study reported that dose-dependent biphasic effects of the HIF-PHD inhibitor on tubule-interstitium fibrosis were observed in CKD mice[92]; (3) the timing of HIF-PHD inhibitor administration will also have an influence. Studies have shown that pre-treatment with an HIF-PHD inhibitor has an anti-fibrotic effect, while the administration of an HIF-PHD inhibitor has different effects on the different stages of fibrosis progression: early long-term treatment exacerbates fibrosis, medium-term treatment alleviates fibrosis, and end-stage treatment has no effect[85]; (4) HIF may play different roles in different renal cells. For example, elevated endothelial HIF-1α contributes to initial glomerular injury, leading to hypertension and progression of renal fibrosis[93], whereas endothelial cell-specific ablation of HIF-1α has no influence on renal function and expression of adhesion molecules, during fibrosis development after unilateral ureteral obstruction[94]. It should be noticed that pharmacological inhibitors generally affect all cell types in the kidneys, while inhibition of HIF by genetic methods only affects specific renal cell types that may contribute distinctly during renal fibrogenesis[89].

Thus, the net balance of beneficial and potential adverse effects of HIF activation may have to be carefully established under conditions of long-term intervention.

5. Conclusions

In summary, we demonstrated that ROX remarkably ameliorated TAC-induced kidney injury *via* reduced TAC, which caused tubule-interstitium fibrosis, glomerulosclerosis, and inflammation, thereby improving kidney function. As per our knowledge, this is the first report on the effect of ROX on the TAC-induced nephrotoxicity rat. Therefore, our findings offered a clinical potential approach for the treatment of TAC-induced nephrotoxicity.

Summary

Chapter 1. Establishment of an experimental rat model of TAC-induced kidney injury accompanied by interstitial fibrosis

Nephrotoxicity is the major adverse reaction to TAC; however, the underlying mechanisms remain to be fully elucidated. Although several TAC-induced nephrotoxicity animal models have been reported, most renal injury rat models contain factors other than TAC. This chapter aimed to develop a new rat model for nephrotoxicity with interstitial fibrosis that was induced by means of TAC administration.

Thirty Wistar rats were randomly divided into four groups: sham-operated (sham), vehicle-treated with I/R injury (I/R), TAC treated (TAC) and TAC treated with I/R injury (TAC+I/R). Rats subjected to I/R injury and treated with TAC for 2 weeks showed higher Scr, BUN, as well as serum Mg and K levels, indicating decreased renal function. In addition, TAC treatment combined with I/R injury increased histological injury (tubular vacuolation, glomerulosclerosis, and interstitial fibrosis), as well as α-SMA, TGF-β, and KIM-1 expression in the renal cortex.

In summary, we developed a TAC-induced kidney injury rat model with interstitial fibrosis within 2 weeks, by creating conditions that mimicked renal transplantation, *via* TAC administration following I/R.

Chapter 2. Effect of ROX in the TAC-induced nephrotoxicity rat model

Tubulo-interstitial hypoxia is considered to be a common pathway for progressive kidney disease. ROX is an oral HIF-PHD inhibitor, that can stabilize HIF and increase iron utilization, thereby stimulating erythropoietin production, and thus, is used as a novel treatment for anemia of CKD. Although it has been demonstrated that ROX ameliorates AKI-induced kidney fibrosis, the effects of ROX in TAC-induced kidney fibrosis have not been explored. This chapter aimed to investigate the effect of ROX on the TAC-induced nephrotoxicity rat.

To assess the anti-fibrotic effect of ROX against TAC-induced kidney fibrosis, ROX (3 mg/kg every 2d) or vehicle (20% DMSO) were gavage administered to male Wistar rats, two days before bilateral renal ischemia (45 min), for 16 d. After bilateral renal ischemia (45 min), TAC (5 mg/kg per day) or saline were subcutaneously administered for 2 weeks.

TAC administration increased Scr, BUN, and KIM-1 levels as well as kidney injuries, such as tubular dilation, vacuolization, renal interstitial fibrosis, glomerulosclerosis, and inflammation in the rats. ROX administration attenuated TAC-induced kidney fibrosis and the associated abnormalities.

We demonstrated that ROX attenuates TAC-induced renal interstitial fibrosis in rats. Because of the protective effect of ROX against TAC-induced kidney fibrosis, ROX may serve to be useful when used concomitantly with TAC.

References

1. Leeson, S.; Desai, S. P., Medical and ethical challenges during the first successful human kidney transplantation in 1954 at Peter Bent Brigham Hospital, Boston. *Anesth Analg* **2015,** *120* (1), 239-245.

2. Kino, T.; Hatanaka, H.; Miyata, S.; Inamura, N.; Nishiyama, M.; Yajima, T.; Goto, T.; Okuhara, M.; Kohsaka, M.; Aoki, H.; et al., FK-506, a novel immunosuppressant isolated from a Streptomyces. II. Immunosuppressive effect of FK-506 in vitro. *The Journal of antibiotics* **1987,** *40* (9), 1256-65.

3. Hatanaka, H.; Iwami, M.; Kino, T.; Goto, T.; Okuhara, M., FR-900520 and FR-900523, novel immunosuppressants isolated from a Streptomyces. I. Taxonomy of the producing strain. *The Journal of antibiotics* **1988,** *41* (11), 1586-91.

4. Shihab, F.; Christians, U.; Smith, L.; Wellen, J. R.; Kaplan, B., Focus on mTOR inhibitors and tacrolimus in renal transplantation: pharmacokinetics, exposure-response relationships, and clinical outcomes. *Transplant immunology* **2014,** *31* (1), 22-32.

5. Jia, J. J.; Lin, B. Y.; He, J. J.; Geng, L.; Kadel, D.; Wang, L.; Yu, D. D.; Shen, T.; Yang, Z.; Ye, Y. F.; Zhou, L.; Zheng, S. S., "Minimizing tacrolimus" strategy and long-term survival after liver transplantation. *World journal of gastroenterology* **2014,** *20* (32), 11363-9.

6. Helmschrott, M.; Beckendorf, J.; Akyol, C.; Ruhparwar, A.; Schmack, B.; Erbel, C.; Gleissner, C. A.; Akhavanpoor, M.; Ehlermann, P.; Bruckner, T.; Katus, H. A.; Doesch, A. O., Superior rejection profile during the first 24 months after heart transplantation under tacrolimus as baseline immunosuppressive regimen. *Drug design, development and therapy* **2014,** *8*, 1307-14.

7. Liu, J.; Farmer, J. D., Jr.; Lane, W. S.; Friedman, J.; Weissman, I.; Schreiber, S. L., Calcineurin is a common target of cyclophilin-cyclosporin A and FKBP-FK506 complexes. *Cell* **1991,** *66* (4), 807-15.

8. Liu, J.; Albers, M. W.; Wandless, T. J.; Luan, S.; Alberg, D. G.; Belshaw, P. J.; Cohen, P.; MacKintosh, C.; Klee, C. B.; Schreiber, S. L., Inhibition of T cell signaling by immunophilin-ligand complexes correlates with

loss of calcineurin phosphatase activity. *Biochemistry* **1992,** *31* (16), 3896-901.

9. Schreiber, S. L.; Crabtree, G. R., The mechanism of action of cyclosporin A and FK506. *Immunology today* **1992,** *13* (4), 136-42.

10. Hogan, P. G.; Chen, L.; Nardone, J.; Rao, A., Transcriptional regulation by calcium, calcineurin, and NFAT. *Genes & development* **2003,** *17* (18), 2205-32.

11. Macian, F., NFAT proteins: key regulators of T-cell development and function. *Nature reviews. Immunology* **2005,** *5* (6), 472-84.

12. Müller, M. R.; Rao, A., NFAT, immunity and cancer: a transcription factor comes of age. *Nature reviews. Immunology* **2010,** *10* (9), 645-56.

13. Staatz, C. E.; Tett, S. E., Clinical pharmacokinetics and pharmacodynamics of tacrolimus in solid organ transplantation. *Clinical pharmacokinetics* **2004,** *43* (10), 623-53.

14. Brunet, M.; van Gelder, T.; Åsberg, A.; Haufroid, V.; Hesselink, D. A.; Langman, L.; Lemaitre, F.; Marquet, P.; Seger, C.; Shipkova, M.; Vinks, A.; Wallemacq, P.; Wieland, E.; Woillard, J. B.; Barten, M. J.;

Budde, K.; Colom, H.; Dieterlen, M. T.; Elens, L.; Johnson-Davis, K. L.; Kunicki, P. K.; MacPhee, I.; Masuda, S.; Mathew, B. S.; Millán, O.; Mizuno, T.; Moes, D. A. R.; Monchaud, C.; Noceti, O.; Pawinski, T.; Picard, N.; van Schaik, R.; Sommerer, C.; Vethe, N. T.; de Winter, B.; Christians, U.; Bergan, S., Therapeutic Drug Monitoring of Tacrolimus-Personalized Therapy: Second Consensus Report. *Therapeutic drug monitoring* **2019,** *41* (3), 261-307.

15. Oetting, W. S.; Wu, B.; Schladt, D. P.; Guan, W.; van Setten, J.; Keating, B. J.; Iklé, D.; Remmel, R. P.; Dorr, C. R.; Mannon, R. B.; Matas, A. J.; Israni, A. K.; Jacobson, P. A., Genetic Variants Associated With Immunosuppressant Pharmacokinetics and Adverse Effects in the DeKAF Genomics Genome-wide Association Studies. *Transplantation* **2019,** *103* (6), 1131-1139.

16. Stegall, M. D.; Cornell, L. D.; Park, W. D.; Smith, B. H.; Cosio, F. G., Renal Allograft Histology at 10 Years After Transplantation in the Tacrolimus Era: Evidence of Pervasive Chronic Injury. *American journal of transplantation :*

official journal of the American Society of Transplantation and the American Society of Transplant Surgeons **2018,** *18* (1), 180-188.

17. Chapman, J. R., Chronic calcineurin inhibitor nephrotoxicity-lest we forget. *American journal of transplantation : official journal of the American Society of Transplantation and the American Society of Transplant Surgeons* **2011,** *11* (4), 693-7.

18. Thannickal, V. J., Aging, antagonistic pleiotropy and fibrotic disease. *Int J Biochem Cell Biol* **2010,** *42* (9), 1398-400.

19. Louis, K.; Hertig, A., How tubular epithelial cells dictate the rate of renal fibrogenesis? *World journal of nephrology* **2015,** *4* (3), 367-73.

20. Simon, N.; Hertig, A., Alteration of Fatty Acid Oxidation in Tubular Epithelial Cells: From Acute Kidney Injury to Renal Fibrogenesis. *Front Med (Lausanne)* **2015,** *2*, 52.

21. Hodgkins, K. S.; Schnaper, H. W., Tubulointerstitial injury and the progression of chronic kidney disease. *Pediatric nephrology (Berlin, Germany)* **2012,** *27* (6), 901-9.

22. Kawakami, T.; Mimura, I.; Shoji, K.; Tanaka, T.; Nangaku, M., Hypoxia and fibrosis in chronic kidney disease: crossing at pericytes. In *Kidney Int Suppl (2011)*, 2014; Vol. 4, pp 107-112.

23. Nangaku, M.; Eckardt, K. U., Hypoxia and the HIF system in kidney disease. *J Mol Med (Berl)* **2007,** *85* (12), 1325-30.

24. Kabei, K.; Tateishi, Y.; Shiota, M.; Osada-Oka, M.; Nishide, S.; Uchida, J.; Nakatani, T.; Matsunaga, S.; Yamaguchi, T.; Tomita, S.; Miura, K., Effects of orally active hypoxia inducible factor alpha prolyl hydroxylase inhibitor, FG4592 on renal fibrogenic potential in mouse unilateral ureteral obstruction model. *J Pharmacol Sci* **2020,** *142* (3), 93-100.

25. Del Balzo, U.; Signore, P. E.; Walkinshaw, G.; Seeley, T. W.; Brenner, M. C.; Wang, Q.; Guo, G.; Arend, M. P.; Flippin, L. A.; Chow, F. A.; Gervasi, D. C.; Kjaergaard, C. H.; Langsetmo, I.; Guenzler, V.; Liu, D. Y.; Klaus, S. J.; Lin, A.; Neff, T. B., Nonclinical Characterization of the Hypoxia-Inducible Factor Prolyl Hydroxylase Inhibitor Roxadustat, a Novel Treatment of Anemia of Chronic Kidney Disease. *The Journal of pharmacology*

and experimental therapeutics **2020,** *374* (2), 342-353.

26. Fang, Y.; Yu, X.; Liu, Y.; Kriegel, A. J.; Heng, Y.; Xu, X.; Liang, M.; Ding, X., miR-29c is downregulated in renal interstitial fibrosis in humans and rats and restored by HIF-α activation. *American journal of physiology. Renal physiology* **2013,** *304* (10), F1274-82.

27. Deng, A.; Arndt, M. A.; Satriano, J.; Singh, P.; Rieg, T.; Thomson, S.; Tang, T.; Blantz, R. C., Renal protection in chronic kidney disease: hypoxia-inducible factor activation vs. angiotensin II blockade. *American journal of physiology. Renal physiology* **2010,** *299* (6), F1365-73.

28. Song, Y. R.; You, S. J.; Lee, Y. M.; Chin, H. J.; Chae, D. W.; Oh, Y. K.; Joo, K. W.; Han, J. S.; Na, K. Y., Activation of hypoxia-inducible factor attenuates renal injury in rat remnant kidney. *Nephrology, dialysis, transplantation : official publication of the European Dialysis and Transplant Association - European Renal Association* **2010,** *25* (1), 77-85.

29. Tanaka, T.; Kojima, I.; Ohse, T.; Ingelfinger, J. R.; Adler, S.; Fujita, T.; Nangaku, M., Cobalt promotes angiogenesis via hypoxia-inducible

factor and protects tubulointerstitium in the remnant kidney model. *Lab Invest* **2005,** *85* (10), 1292-307.

30. Kobayashi, H.; Gilbert, V.; Liu, Q.; Kapitsinou, P. P.; Unger, T. L.; Rha, J.; Rivella, S.; Schlöndorff, D.; Haase, V. H., Myeloid cell-derived hypoxia-inducible factor attenuates inflammation in unilateral ureteral obstruction-induced kidney injury. *J Immunol* **2012,** *188* (10), 5106-15.

31. Oh, S. W.; Ahn, J. M.; Lee, Y. M.; Kim, S.; Chin, H. J.; Chae, D. W.; Na, K. Y., Activation of hypoxia-inducible factor by cobalt is associated with the attenuation of tissue injury and apoptosis in cyclosporine-induced nephropathy. *Tohoku J Exp Med* **2012,** *226* (3), 197-206.

32. Wu, M.; Chen, W.; Miao, M.; Jin, Q.; Zhang, S.; Bai, M.; Fan, J.; Zhang, Y.; Zhang, A.; Jia, Z.; Huang, S., Anti-anemia drug FG4592 retards the AKI-to-CKD transition by improving vascular regeneration and antioxidative capability. *Clin Sci (Lond)* **2021,** *135* (14), 1707-1726.

33. Li, X.; Zou, Y.; Xing, J.; Fu, Y. Y.; Wang, K. Y.; Wan, P. Z.; Zhai, X. Y., Pretreatment with Roxadustat (FG-4592) Attenuates Folic Acid-Induced

Kidney Injury through Antiferroptosis via Akt/GSK-3β/Nrf2 Pathway. *Oxid Med Cell Longev* **2020,** *2020*, 6286984.

34. Naesens, M.; Kuypers, D. R.; Sarwal, M., Calcineurin inhibitor nephrotoxicity. *Clinical journal of the American Society of Nephrology : CJASN* **2009,** *4* (2), 481-508.

35. Vandenbussche, C.; Van der Hauwaert, C.; Dewaeles, E.; Franczak, J.; Hennino, M. F.; Gnemmi, V.; Savary, G.; Tavernier, Q.; Nottet, N.; Paquet, A.; Perrais, M.; Blum, D.; Mari, B.; Pottier, N.; Glowacki, F.; Cauffiez, C., Tacrolimus-induced nephrotoxicity in mice is associated with microRNA deregulation. *Arch Toxicol* **2018,** *92* (4), 1539-1550.

36. Lim, S. W.; Jin, L.; Luo, K.; Jin, J.; Shin, Y. J.; Hong, S. Y.; Yang, C. W., Klotho enhances FoxO3-mediated manganese superoxide dismutase expression by negatively regulating PI3K/AKT pathway during tacrolimus-induced oxidative stress. *Cell death & disease* **2017,** *8* (8), e2972.

37. Sanchez-Campos, S.; Lopez-Acebo, R.; Gonzalez, P.; Culebras, J. M.; Tuñon, M. J.; Gonzalez-Gallego, J., Cholestasis and alterations of

glutathione metabolism induced by tacrolimus (FK506) in the rat. *Transplantation* **1998,** *66* (1), 84-8.

38. Shihab, F. S.; Bennett, W. M.; Tanner, A. M.; Andoh, T. F., Mechanism of fibrosis in experimental tacrolimus nephrotoxicity. *Transplantation* **1997,** *64* (12), 1829-37.

39. Cockfield, S. M.; Wilson, S.; Campbell, P. M.; Cantarovich, M.; Gangji, A.; Houde, I.; Jevnikar, A. M.; Keough-Ryan, T. M.; Monroy-Cuadros, F. M.; Nickerson, P. W.; Pâquet, M. R.; Ramesh Prasad, G. V.; Senécal, L.; Shoker, A.; Wolff, J. L.; Howell, J.; Schwartz, J. J.; Rush, D. N., Comparison of the effects of standard vs low-dose prolonged-release tacrolimus with or without ACEi/ARB on the histology and function of renal allografts. *American journal of transplantation : official journal of the American Society of Transplantation and the American Society of Transplant Surgeons* **2019,** *19* (6), 1730-1744.

40. Prókai, Á.; Csohány, R.; Sziksz, E.; Pap, D.; Balicza-Himer, L.; Boros, S.; Magda, B.; Vannay, Á.; Kis-Petik, K.; Fekete, A.; Peti-Peterdi,

J.; Szabó, A. J., Calcineurin-inhibition Results in Upregulation of Local Renin and Subsequent Vascular Endothelial Growth Factor Production in Renal Collecting Ducts. *Transplantation* **2016,** *100* (2), 325-333.

41. Kidokoro, K.; Satoh, M.; Nagasu, H.; Sakuta, T.; Kuwabara, A.; Yorimitsu, D.; Nishi, Y.; Tomita, N.; Sasaki, T.; Kashihara, N., Tacrolimus induces glomerular injury via endothelial dysfunction caused by reactive oxygen species and inflammatory change. *Kidney & blood pressure research* **2012,** *35* (6), 549-57.

42. Andoh, T. F.; Burdmann, E. A.; Lindsley, J.; Houghton, D. C.; Bennett, W. M., Functional and structural characteristics of experimental FK 506 nephrotoxicity. *Clinical and experimental pharmacology & physiology* **1995,** *22* (9), 646-54.

43. Andoh, T. F.; Burdmann, E. A.; Lindsley, J.; Houghton, D. C.; Bennett, W. M., Enhancement of FK506 nephrotoxicity by sodium depletion in an experimental rat model. *Transplantation* **1994,** *57* (4), 483-9.

44. Gonçalves, G. M.; Cenedeze, M. A.; Feitoza, C. Q.; Wang, P. M.;

Bertocchi, A. P.; Damião, M. J.; Pinheiro, H. S.; Antunes Teixeira, V. P.; dos Reis, M. A.; Pacheco-Silva, A.; Câmara, N. O., The role of heme oxygenase 1 in rapamycin-induced renal dysfunction after ischemia and reperfusion injury. *Kidney international* **2006,** *70* (10), 1742-9.

45. Roufosse, C.; Simmonds, N.; Clahsen-van Groningen, M.; Haas, M.; Henriksen, K. J.; Horsfield, C.; Loupy, A.; Mengel, M.; Perkowska-Ptasińska, A.; Rabant, M.; Racusen, L. C.; Solez, K.; Becker, J. U., A 2018 Reference Guide to the Banff Classification of Renal Allograft Pathology. *Transplantation* **2018,** *102* (11), 1795-1814.

46. Cosner, D.; Zeng, X.; Zhang, P. L., Proximal Tubular Injury in Medullary Rays Is an Early Sign of Acute Tacrolimus Nephrotoxicity. *Journal of transplantation* **2015,** *2015*, 142521.

47. McGrath, J. S.; Shehata, M., The effect of differing immunosuppressive regimes on the functional and morphologic changes in a rat renal allograft model of chronic rejection. *Transplantation proceedings* **2001,** *33* (3), 2191-2.

48. Rosen, S.; Greenfeld, Z.; Brezis, M., Chronic cyclosporine-induced

nephropathy in the rat. A medullary ray and inner stripe injury. *Transplantation* **1990,** *49* (2), 445-52.

49. Maluccio, M.; Sharma, V.; Lagman, M.; Vyas, S.; Yang, H.; Li, B.; Suthanthiran, M., Tacrolimus enhances transforming growth factor-beta1 expression and promotes tumor progression. *Transplantation* **2003,** *76* (3), 597-602.

50. Akool el, S.; Doller, A.; Babelova, A.; Tsalastra, W.; Moreth, K.; Schaefer, L.; Pfeilschifter, J.; Eberhardt, W., Molecular mechanisms of TGF beta receptor-triggered signaling cascades rapidly induced by the calcineurin inhibitors cyclosporin A and FK506. *J Immunol* **2008,** *181* (4), 2831-45.

51. Khanna, A.; Plummer, M.; Bromberek, C.; Bresnahan, B.; Hariharan, S., Expression of TGF-beta and fibrogenic genes in transplant recipients with tacrolimus and cyclosporine nephrotoxicity. *Kidney international* **2002,** *62* (6), 2257-63.

52. Roos-van Groningen, M. C.; Scholten, E. M.; Lelieveld, P. M.; Rowshani, A. T.; Baelde, H. J.; Bajema, I. M.; Florquin, S.; Bemelman, F.

J.; de Heer, E.; de Fijter, J. W.; Bruijn, J. A.; Eikmans, M., Molecular comparison of calcineurin inhibitor-induced fibrogenic responses in protocol renal transplant biopsies. *Journal of the American Society of Nephrology : JASN* **2006,** *17* (3), 881-8.

53. Ichimura, T.; Bonventre, J. V.; Bailly, V.; Wei, H.; Hession, C. A.; Cate, R. L.; Sanicola, M., Kidney injury molecule-1 (KIM-1), a putative epithelial cell adhesion molecule containing a novel immunoglobulin domain, is up-regulated in renal cells after injury. *The Journal of biological chemistry* **1998,** *273* (7), 4135-42.

54. Huo, W.; Zhang, K.; Nie, Z.; Li, Q.; Jin, F., Kidney injury molecule-1 (KIM-1): a novel kidney-specific injury molecule playing potential double-edged functions in kidney injury. *Transplant Rev (Orlando)* **2010,** *24* (3), 143-6.

55. Bansal, N.; Carpenter, M. A.; Weiner, D. E.; Levey, A. S.; Pfeffer, M.; Kusek, J. W.; Cai, J.; Hunsicker, L. G.; Park, M.; Bennett, M.; Liu, K. D.; Hsu, C. Y., Urine Injury Biomarkers and Risk of Adverse Outcomes in Recipients of Prevalent Kidney Transplants: The Folic Acid for Vascular Outcome

Reduction in Transplantation Trial. *Journal of the American Society of Nephrology : JASN* **2016,** *27* (7), 2109-21.

56. Humphreys, B. D.; Xu, F.; Sabbisetti, V.; Grgic, I.; Movahedi Naini, S.; Wang, N.; Chen, G.; Xiao, S.; Patel, D.; Henderson, J. M.; Ichimura, T.; Mou, S.; Soeung, S.; McMahon, A. P.; Kuchroo, V. K.; Bonventre, J. V., Chronic epithelial kidney injury molecule-1 expression causes murine kidney fibrosis. *The Journal of clinical investigation* **2013,** *123* (9), 4023-35.

57. Vaidya, V. S.; Ramirez, V.; Ichimura, T.; Bobadilla, N. A.; Bonventre, J. V., Urinary kidney injury molecule-1: a sensitive quantitative biomarker for early detection of kidney tubular injury. *American journal of physiology. Renal physiology* **2006,** *290* (2), F517-29.

58. Nogare, A. L.; Veronese, F. V.; Carpio, V. N.; Montenegro, R. M.; Pedroso, J. A.; Pegas, K. L.; Gonçalves, L. F.; Manfro, R. C., Kidney injury molecule-1 expression in human kidney transplants with interstitial fibrosis and tubular atrophy. *BMC nephrology* **2015,** *16*, 19.

59. Shinke, H.; Masuda, S.; Togashi, Y.; Ikemi, Y.; Ozawa, A.; Sato, T.; Kim, Y. H.; Mishima, M.; Ichimura, T.; Bonventre, J. V.; Matsubara, K., Urinary kidney injury molecule-1 and monocyte chemotactic protein-1 are noninvasive biomarkers of cisplatin-induced nephrotoxicity in lung cancer patients. *Cancer chemotherapy and pharmacology* **2015,** *76* (5), 989-96.

60. Segarra-Medrano, A.; Carnicer-Caceres, C.; Valtierra-Carmeno, N.; Agraz-Pamplona, I.; Ramos-Terrades, N.; Jatem Escalante, E.; Ostos-Roldan, E., Value of urinary levels of interleukin-6, epidermal growth factor, monocyte chemoattractant protein type1 and transforming growth factor β1 in predicting the extent of fibrosis lesions in kidney biopsies of patients with IgA nephropathy. *Nefrologia : publicacion oficial de la Sociedad Espanola Nefrologia* **2017,** *37* (5), 531-538.

61. Coca, S. G.; Singanamala, S.; Parikh, C. R., Chronic kidney disease after acute kidney injury: a systematic review and meta-analysis. *Kidney international* **2012,** *81* (5), 442-8.

62. Hongtao, C.; Youling, F.; Fang, H.; Huihua, P.; Jiying, Z.; Jun, Z.,

Curcumin alleviates ischemia reperfusion-induced late kidney fibrosis through the APPL1/Akt signaling pathway. *J Cell Physiol* **2018,** *233* (11), 8588-8596.

63. Piao, Y.; Liu, Y.; Xie, X., Change trends of organ weight background data in sprague dawley rats at different ages. *J Toxicol Pathol* **2013,** *26* (1), 29-34.

64. Venkataramanan, R.; Swaminathan, A.; Prasad, T.; Jain, A.; Zuckerman, S.; Warty, V.; McMichael, J.; Lever, J.; Burckart, G.; Starzl, T., Clinical pharmacokinetics of tacrolimus. *Clinical pharmacokinetics* **1995,** *29* (6), 404-30.

65. Jiang, H.; Sakuma, S.; Fujii, Y.; Akiyama, Y.; Ogawa, T.; Tamura, K.; Kobayashi, M.; Fujitsu, T., Tacrolimus versus cyclosporin A: a comparative study on rat renal allograft survival. *Transplant international : official journal of the European Society for Organ Transplantation* **1999,** *12* (2), 92-9.

66. Cvetkovic, M.; Mann, G. N.; Romero, D. F.; Liang, X. G.; Ma, Y.; Jee, W. S.; Epstein, S., The deleterious effects of long-term cyclosporine A, cyclosporine G, and FK506 on bone mineral metabolism in vivo. *Transplantation* **1994,** *57* (8), 1231-7.

67. Shu, S.; Wang, Y.; Zheng, M.; Liu, Z.; Cai, J.; Tang, C.; Dong, Z., Hypoxia and Hypoxia-Inducible Factors in Kidney Injury and Repair. *Cells* **2019,** *8* (3).

68. Liu, M.; Ning, X.; Li, R.; Yang, Z.; Yang, X.; Sun, S.; Qian, Q., Signalling pathways involved in hypoxia-induced renal fibrosis. *J Cell Mol Med* **2017,** *21* (7), 1248-1259.

69. Friedman, S. L.; Sheppard, D.; Duffield, J. S.; Violette, S., Therapy for fibrotic diseases: nearing the starting line. *Sci Transl Med* **2013,** *5* (167), 167sr1.

70. Liu, Y., Cellular and molecular mechanisms of renal fibrosis. *Nat Rev Nephrol* **2011,** *7* (12), 684-96.

71. Eddy, A. A., Overview of the cellular and molecular basis of kidney fibrosis. In *Kidney Int Suppl (2011),* 2014; Vol. 4, pp 2-8.

72. Manotham, K.; Tanaka, T.; Matsumoto, M.; Ohse, T.; Inagi, R.; Miyata, T.; Kurokawa, K.; Fujita, T.; Ingelfinger, J. R.; Nangaku, M., Transdifferentiation of cultured tubular cells induced by hypoxia. *Kidney*

international **2004,** *65* (3), 871-80.

73. Fine, L. G.; Norman, J. T., Chronic hypoxia as a mechanism of progression of chronic kidney diseases: from hypothesis to novel therapeutics. *Kidney international* **2008,** *74* (7), 867-72.

74. Norman, J. T.; Fine, L. G., Intrarenal oxygenation in chronic renal failure. *Clinical and experimental pharmacology & physiology* **2006,** *33* (10), 989-96.

75. Mimura, I.; Nangaku, M., The suffocating kidney: tubulointerstitial hypoxia in end-stage renal disease. *Nat Rev Nephrol* **2010,** *6* (11), 667-78.

76. Zafrani, L.; Ince, C., Microcirculation in Acute and Chronic Kidney Diseases. *American journal of kidney diseases : the official journal of the National Kidney Foundation* **2015,** *66* (6), 1083-94.

77. Mayer, G., Capillary rarefaction, hypoxia, VEGF and angiogenesis in chronic renal disease. *Nephrology, dialysis, transplantation : official publication of the European Dialysis and Transplant Association - European Renal Association* **2011,** *26* (4), 1132-7.

78. Barratt, J.; Andric, B.; Tataradze, A.; Schömig, M.; Reusch, M.;

Valluri, U.; Mariat, C., Roxadustat for the treatment of anaemia in chronic kidney disease patients not on dialysis: a Phase 3, randomized, open-label, active-controlled study (DOLOMITES). *Nephrology, dialysis, transplantation : official publication of the European Dialysis and Transplant Association - European Renal Association* **2021,** *36* (9), 1616-1628.

79. Zhang, M.; Dong, R.; Yuan, J.; Da, J.; Zha, Y.; Long, Y., Roxadustat (FG-4592) protects against ischaemia/reperfusion-induced acute kidney injury through inhibiting the mitochondrial damage pathway in mice. *Clinical and experimental pharmacology & physiology* **2022,** *49* (2), 311-318.

80. Miao, A. F.; Liang, J. X.; Yao, L.; Han, J. L.; Zhou, L. J., Hypoxia-inducible factor prolyl hydroxylase inhibitor roxadustat (FG-4592) protects against renal ischemia/reperfusion injury by inhibiting inflammation. *Renal failure* **2021,** *43* (1), 803-810.

81. Li, X.; Jiang, B.; Zou, Y.; Zhang, J.; Fu, Y. Y.; Zhai, X. Y., Roxadustat (FG-4592) Facilitates Recovery From Renal Damage by Ameliorating Mitochondrial Dysfunction Induced by Folic Acid. *Frontiers in pharmacology*

2021, *12*, 788977.

82. Yang, Y.; Yu, X.; Zhang, Y.; Ding, G.; Zhu, C.; Huang, S.; Jia, Z.; Zhang, A., Hypoxia-inducible factor prolyl hydroxylase inhibitor roxadustat (FG-4592) protects against cisplatin-induced acute kidney injury. *Clin Sci (Lond)* 2018, *132* (7), 825-838.

83. Beck, J.; Henschel, C.; Chou, J.; Lin, A.; Del Balzo, U., Evaluation of the Carcinogenic Potential of Roxadustat (FG-4592), a Small Molecule Inhibitor of Hypoxia-Inducible Factor Prolyl Hydroxylase in CD-1 Mice and Sprague Dawley Rats. *Int J Toxicol* 2017, *36* (6), 427-439.

84. Gupta, N.; Wish, J. B., Hypoxia-Inducible Factor Prolyl Hydroxylase Inhibitors: A Potential New Treatment for Anemia in Patients With CKD. *American journal of kidney diseases : the official journal of the National Kidney Foundation* 2017, *69* (6), 815-826.

85. Yu, X.; Fang, Y.; Liu, H.; Zhu, J.; Zou, J.; Xu, X.; Jiang, S.; Ding, X., The balance of beneficial and deleterious effects of hypoxia-inducible factor activation by prolyl hydroxylase inhibitor in rat remnant kidney depends on

the timing of administration. *Nephrology, dialysis, transplantation : official publication of the European Dialysis and Transplant Association - European Renal Association* **2012,** *27* (8), 3110-9.

86. Conde, E.; Alegre, L.; Blanco-Sánchez, I.; Sáenz-Morales, D.; Aguado-Fraile, E.; Ponte, B.; Ramos, E.; Sáiz, A.; Jiménez, C.; Ordoñez, A.; López-Cabrera, M.; del Peso, L.; de Landázuri, M. O.; Liaño, F.; Selgas, R.; Sanchez-Tomero, J. A.; García-Bermejo, M. L., Hypoxia inducible factor 1-alpha (HIF-1 alpha) is induced during reperfusion after renal ischemia and is critical for proximal tubule cell survival. *PloS one* **2012,** *7* (3), e33258.

87. Tanaka, T.; Kojima, I.; Ohse, T.; Inagi, R.; Miyata, T.; Ingelfinger, J. R.; Fujita, T.; Nangaku, M., Hypoxia-inducible factor modulates tubular cell survival in cisplatin nephrotoxicity. *American journal of physiology. Renal physiology* **2005,** *289* (5), F1123-33.

88. Wang, W. W.; Li, Z. Z.; Wang, W.; Jiang, Y.; Cheng, J.; Lu, S.; Zhang, J. Y., Enhanced renoprotective effect of HIF-1 α modified human adipose-derived stem cells on cisplatin-induced acute kidney injury in vivo. *Scientific*

reports **2015,** *5*, 10851.

89. Liu, J.; Wei, Q.; Guo, C.; Dong, G.; Liu, Y.; Tang, C.; Dong, Z., Hypoxia, HIF, and Associated Signaling Networks in Chronic Kidney Disease. *International journal of molecular sciences* **2017,** *18* (5).

90. Kapitsinou, P. P.; Sano, H.; Michael, M.; Kobayashi, H.; Davidoff, O.; Bian, A.; Yao, B.; Zhang, M. Z.; Harris, R. C.; Duffy, K. J.; Erickson-Miller, C. L.; Sutton, T. A.; Haase, V. H., Endothelial HIF-2 mediates protection and recovery from ischemic kidney injury. *The Journal of clinical investigation* **2014,** *124* (6), 2396-409.

91. Kong, K. H.; Oh, H. J.; Lim, B. J.; Kim, M.; Han, K. H.; Choi, Y. H.; Kwon, K.; Nam, B. Y.; Park, K. S.; Park, J. T.; Han, S. H.; Yoo, T. H.; Lee, S.; Kim, S. J.; Kang, D. H.; Choi, K. B.; Eremina, V.; Quaggin, S. E.; Ryu, D. R.; Kang, S. W., Selective tubular activation of hypoxia-inducible factor-2 α has dual effects on renal fibrosis. *Scientific reports* **2017,** *7* (1), 11351.

92. Li, Z. L.; Lv, L. L.; Wang, B.; Tang, T. T.; Feng, Y.; Cao, J. Y.; Jiang, L. Q.; Sun, Y. B.; Liu, H.; Zhang, X. L.; Ma, K. L.; Tang, R. N.; Liu,

B. C., The profibrotic effects of MK-8617 on tubulointerstitial fibrosis mediated by the KLF5 regulating pathway. *Faseb j* **2019,** *33* (11), 12630-12643.

93. Luo, R.; Zhang, W.; Zhao, C.; Zhang, Y.; Wu, H.; Jin, J.; Grenz, A.; Eltzschig, H. K.; Tao, L.; Kellems, R. E.; Xia, Y., Elevated Endothelial Hypoxia-Inducible Factor-1 α Contributes to Glomerular Injury and Promotes Hypertensive Chronic Kidney Disease. *Hypertension* **2015,** *66* (1), 75-84.

94. Kalucka, J.; Schley, G.; Georgescu, A.; Klanke, B.; Rössler, S.; Baumgartl, J.; Velden, J.; Amann, K.; Willam, C.; Johnson, R. S.; Eckardt, K. U.; Weidemann, A., Kidney injury is independent of endothelial HIF-1 α . *J Mol Med (Berl)* **2015,** *93* (8), 891-904.

Acknowledgments

Foremost, I would like to express my sincere gratitude to my supervisors Dr. Ieiri and Dr. Egashira for their continuous guidance and mentorship throughout my Ph.D. study. I also would like to thank Dr. Tajima for his guidance, and support throughout my research and writing of this thesis.

My appreciation also extends to all the members in my laboratory for their kind help and support with my research.

I thank MEXT and Kyushu University for offering me the opportunity to pursue research in Japan. This experience will be a precious and unforgettable memory for me, and I look forward to coming back here again someday in the future.

Last but not the least, I would like to thank my family for their love and unwavering support throughout my life; without them none of this would have been possible. My special thanks go to my friend, Cheng Chen, for being with me and for filling my life with happiness.